Tetrahedron 67 (2011) 3573–3601

Contents lists available at ScienceDirect

Tetrahedron

journal homepage: www.elsevier.com/locate/tet

Tetrahedron report number 939

4,4′-Difluoro-4-bora-3a,4a-diaza-*s*-indacenes (BODIPYs) as components of novel light active materials

Michael Benstead, Georg H. Mehl, Ross W. Boyle *

Department of Chemistry, University of Hull, Kingston-upon-Hull, East Yorkshire HU6 7RX, UK

ARTICLE INFO

Article history:
Received 1 March 2011
Available online 17 March 2011

Contents

1. Introduction

4,4-Difluoro-4-bora-3a,4a-diaza-*s*-indacenes (hereafter referred to as BODIPYs) are a class of fluorescent dyes that are finding an increasing number of applications in both the materials and optical imaging fields. BODIPYs have a sharp fluorescence profile, high degree of photostability and can have fluorescence quantum yields approaching unity, depending on the attached substituents.

Abbreviations: ANT, Anthracene; BHJ, bulk-heterojunction solar cell; BODIPY/BDP,4′-Difluoro-4-bora-3a,4a-diaza-*s*-indacene, 4; CDB, Cumyl dithiobenzoate; Col_h, hexagonal columnar; CS, charge-separated state; DABCO, 1,4-Diazabicyclo[2.2.2]octane; DMAEMA, 2-(Dimethylamino)ethyl methacrylate; DSSC, dye-sensitised solar cell; EDOT, 3,4-Ethylenedioxythiophene; EGDMA, Ethylene glycol dimethylacrylate; FRET, fluorescence/förster resonance energy transfer; FTO, fluorinated tin oxide; HEMA, hydroxyethyl methacrylate; HFMA, 2,2,3,3,4,4,4-Heptafluorobutyl methacrylate; HOMO, highest occupied molecular orbital; ITO, Indium-tin oxide; LUMO, lowest occupied molecular orbital; MeTMOS, Methyltrimethoxysilane; MLCTtransfer, metal-to-ligand charge; MMA, Methyl methacrylate; OLED, organic light emitting diode; PCBM, [6,6]-Phenyl-C_{61}-butyric acid methyl ester; PCE, power conversion efficiency; PDI, polydispersity index; PEDOT-PSS, poly(3,4-ethylenedioxythiophene) poly(styrenesulfonate); PEG, poly(ethylene glycol); PETA, Pentaerythritol triacrylate; PETRA, Pentaerythritol tetraacrylate; PFMA, 2,2,3,3,3-Pentafluoropropyl methacrylate; PM, Pyrromethene; PMMA, poly(methyl methacrylate); POLICRYPS, polymer liquid crystal polymer slice; RE, relative efficiency; TEOS, Tetraethyl orthosilicate; TFMA, 2,2,2-Trifluoromethyl methacrylate; TMSPMA, 3-(Trimethoxysilyl)propyl methacrylate.

* Corresponding author. E-mail address: R.W.Boyle@hull.ac.uk (R.W. Boyle).

0040-4020/$ – see front matter
doi:10.1016/j.tet.2011.03.028

BODIPYs and their dipyrrin precursors have been recently reviewed[1–3] with emphasis placed on their syntheses, reactions and applications as fluorescent chemosensors. These reviews outlined the relatively straightforward synthetic routes to the BODIPY fluorophore (Fig. 1), as well as a variety of reliable reactions that can be carried out to produce a shift in the absorption and emission wavelengths. BODIPYs have been used to detect metal cations,[4–12] anions,[13–16] reactive oxygen species[17] and even changes in viscosity[18] by alterations in either the fluorescence intensity or wavelength. Marked changes in the fluorescence intensity as a means of detection are more common and occur because of an ON/OFF switching of photoinduced electron transfer, generally between the BODIPY core and an 8-phenyl substituent. More recently, BODIPY derivatives have been functionalised with groups promoting singlet oxygen generation (e.g., iodide groups), allowing their use as photodynamic therapy agents, an application more commonly associated with porphyrins and phthalocyanines.[19–23] This review, however, focuses on BODIPYs as fluorescent components in materials, and their applications. There is an increasing interest in photonic organic based materials, and BODIPYs are emerging as a unique sub-set of this class of compound, which exhibit novel self-assembly, laser behaviour and highly efficient through-bond and through-space energy transfer.

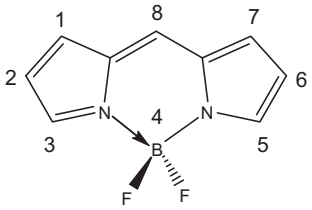

Fig. 1. Core unsubstituted BODIPY.

2. Energy-transfer cassettes

2.1. Through-space energy-transfer cassettes

An energy-transfer cassette consists of two or more fluorescent units attached to the same molecule. The reason for this is that one of these units acts as a donor and the other as an acceptor. The donor absorbs light and this energy is then passed to the acceptor, which emits the light at a longer wavelength. The energy can be transferred to the acceptor via through-space or through-bond energy transfer.

The efficiency of through-space energy transfer depends on the spectral overlap of the donor emission with the acceptor absorbance, the distance between the donor and the acceptor, the relative orientation of donor and acceptor, and the effectiveness of other de-excitation modes (e.g., emission from donor, non-radiative processes). Through-space energy transfer has the effect of artificially enhancing the Stokes' shift of the molecule by causing emission from the acceptor in place of the absorbing (donor) fluorophore. Due to their intense fluorescence, BODIPYs have found uses in the synthesis of new energy-transfer cassettes.

Due to the similarity of their structures, energy-transfer cassettes containing BODIPY and porphyrin units have received a lot of attention for their through-bond energy-transfer processes and subsequent applications as molecular wires. Through-space energy transfer involving porphyrinic units has been less thoroughly investigated. A simple 8-(4-hydroxyphenyl)-BODIPY has been coordinated to an antimony tetraphenylporphyrin (Sb(TPP)) via an alkyl chain to form a through-space energy-transfer cassette. The efficiency of the energy transfer varied between 13 and 40%. By increasing the length of the alkyl chain spacer unit, the efficiency was found to decrease. It was found that the BODIPY acted as the donor and, therefore, no quenching of the excited state of the porphyrin by donation of energy to the BODIPY was found. It was found that quenching did occur when a phenoxy group was coordinated to the other side of the antimony in conjunction with the BODIPY (**1**) (Fig. 2).[24]

A similar compound based on a silicon phthalocyanine has been synthesised, which exhibits competitive energy and electron transfer. Analogous to the antimony–porphyrin–BODIPY array (**1**), when excited at the BODIPY absorption maximum, emission was observed from the phthalocyanine core (**2**) (Fig. 3). The phthalocyanine emission was also observed when the compound was excited at the phthalocyanine core wavelength. However, when a styryl-BODIPY was attached to the silicon centre in the same way, i.e., (**3**), different energy transfer behaviour was observed. When excited at the styryl-BODIPY absorption wavelength, very weak emission from the BODIPY

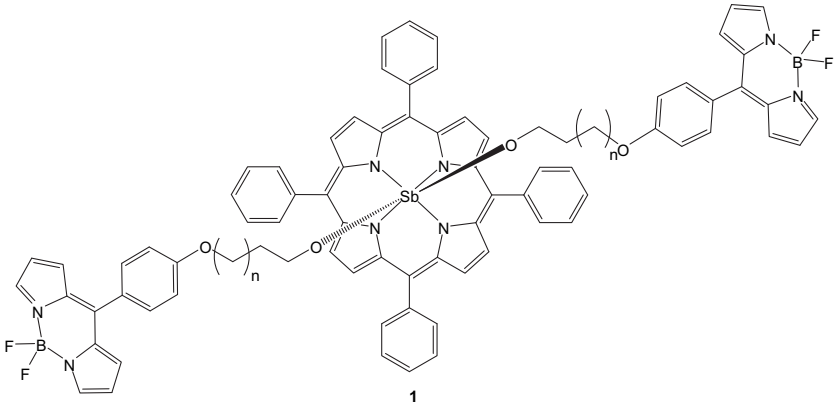

Fig. 2. Antimony–porphyrin–BODIPY array.

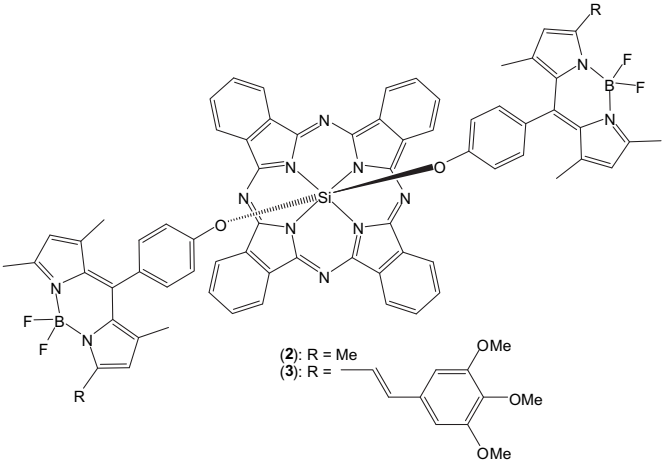

Fig. 3. Di-BODIPY–phthalocyanine array.

and the phthalocyanine was observed. This shows that energy transfer from the BODIPY excited state to the phthalocyanine does occur, but the subsequent emission is largely quenched, presumably by an electron-transfer process. Phthalocyanine fluorescence is also very weak when the molecule is excited at the phthalocyanine excitation wavelength (673 nm). This weak fluorescence would also be due to the same electron-transfer process, as energy transfer from the phthalocyanine to the styryl-BODIPY core is energetically unfavourable. This shows that an electron-transfer process is switched off for the non-styryl-BODIPY analogue upon phthalocyanine excitation, but switched on in the styryl-BODIPY analogue.[25]

Energy transfer to the BODIPY can be achieved through careful selection of both the BODIPY used and the attached fluorophore. Energy transfer from the silicon phthalocyanine to the BODIPY is energetically unfavourable, due to the lower-energy light that is absorbed by the silicon phthalocyanine being unable to promote an electron into the higher energy LUMO of the BODIPY, but, by using a sub-phthalocyanine and a di-styryl-BODIPY, energy transfer to the BODIPY does occur.

For compound **4** (Fig. 4), where only methyl groups are attached to the BODIPY, when excited at 470 nm (partial BODIPY excitation

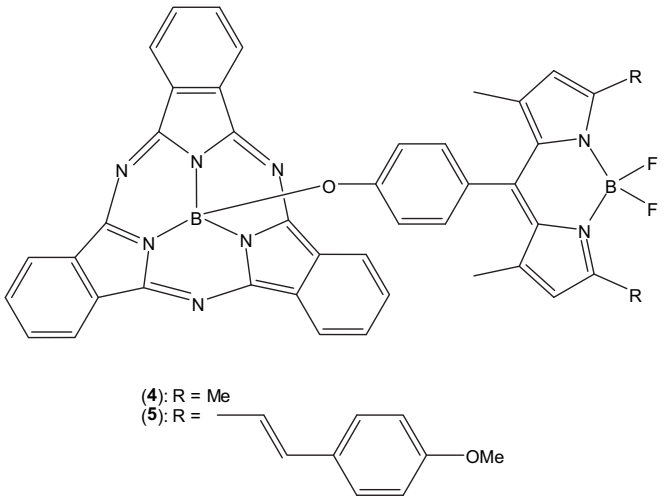

Fig. 4. BODIPY–subphthalocyanine arrays.

avoiding excitation of the boron–subphthalocyanine) energy transfer occurred onto the boron–subphthalocyanine and emission was observed at 570 nm. However, when the di-styryl-BODIPY (**5**) was used, excitation of the sub-phthalocyanine at 515 nm caused energy transfer to the BODIPY and subsequent emission at 653 nm. The energy-transfer quantum yield for both processes was calculated to be 98%.[26]

Through-space energy transfer has also been shown to occur between a BODIPY–zinc porphyrin–phenanthroline and an *N*-unsubstituted imidazole-H_2–porphyrin–phenanthroline system. The imidazole-appended porphyrin is tethered to the zinc-porphyrin–phenanthroline unit by hydrogen bonding between the imidazole NH and two of the phenanthroline nitrogens, as well as a coordinative bond between the zinc(II) centre and the imidazole free nitrogen.[27,28] Despite the lack of any covalent bond between the two units, energy-transfer still occurs from the BODIPY fluorophore to the H_2–porphyrin with a net efficiency of 80%. Energy transfer from the zinc–porphyrin–imidazole complex to the H_2–porphyrin occurred with an efficiency of 85%.

Both energy and electron transfer have been shown to occur sequentially in a BODIPY–zinc-porphyrin–crown ether triad bound to a fulleropyrrolidine.[29] In this triad (**6**) (Fig. 5) energy transfer occurs from the BODIPY to the zinc porphyrin followed by electron transfer from the zinc porphyrin to the fullerene unit. When excited at 495 nm (BODIPY excitation), both emission from the BODIPY and the zinc porphyrin was observed. The emission from the BODIPY core was partially quenched by the energy transfer to the zinc porphyrin with an efficiency of ~97%. A small anodic shift of the zinc porphyrin in the cyclic voltammogram of the triad coordinated to the fullerene, compared to the free triad, indicated interactions between the zinc porphyrin and the fullerene unit.

An energy diagram was constructed showing the various processes involved in this triad system (Fig. 6). As can be seen, the initial step involves excitation of the BODIPY followed by energy transfer to the zinc porphyrin, or this step can be bypassed by directly exciting the zinc porphyrin. This is followed by charge separation to give the mono-cationic zinc porphyrin and the mono-anionic fullerene, which then undergo charge recombination to give the ground state compound again. A small amount of the singlet excited state zinc porphyrin undergoes inter-system crossing to produce the triplet excited zinc porphyrin, which can either

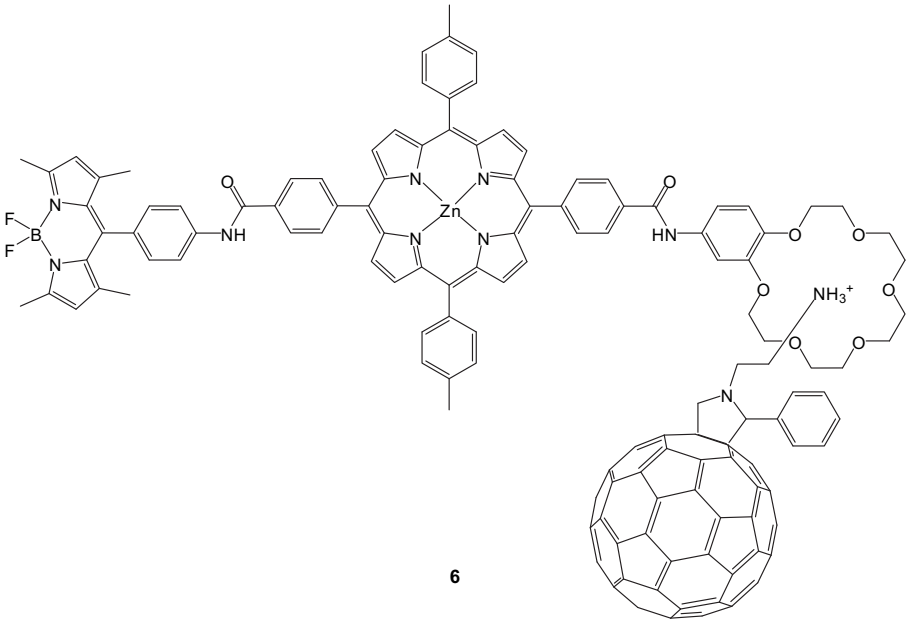

Fig. 5. BODIPY–porphyrin–fullerene array.

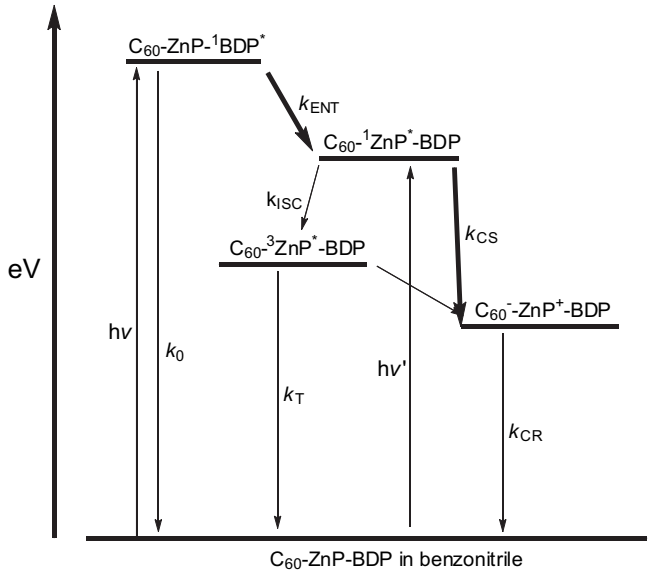

Fig. 6. Energy level diagram showing the different photochemical processes of the BODIPY–zinc-porphyrin–crown ether triad (**6**) when coordinated to the fullerene unit (major processes are bold arrows).

solvent (benzonitrile in this case, when compared to toluene, dichlomethane and methyl-tetrahydrofuran).

Attachment of BODIPYs to a perylenediimide core has become increasingly common and has recently been achieved using click chemistry. This copper(I)-catalysed reaction has been utilized to attach four and six BODIPY 'arms' onto a perylenediimide core, with both compounds showing energy transfer from the BODIPYs to the perylenediimide (**7**) (Fig. 7).[32,33] While the absorption spectrum of the tetra-BODIPY–perylenediimide array shows absorption from the BODIPY and the perylenediimide, the emission spectrum only shows emission from the perylenediimide core, indicating efficient energy transfer (99%). The emission from the perylenediimide core is actually enhanced when excited at the BODIPY absorption wavelength (compared to direct excitation at the perylenediimide core (588 nm)), indicating an 'antenna' effect. A similar effect is seen for the *hexakis*-BODIPY–perylenediimide. Due to the presence of additional BODIPY units, the absorption peak of these units is more intense. That there is a negligible increase in energy transfer when two additional BODIPY units are added supports the theory that BODIPYs are very efficient energy-transfer materials.

Click chemistry has also been used to connect three different BODIPYs together in an energy transfer array (**8**) (Fig. 8).[34] In this array, both BODIPY 'arms' act as donors for the central BODIPY acceptor. The styryl units on the central BODIPY have the effect of

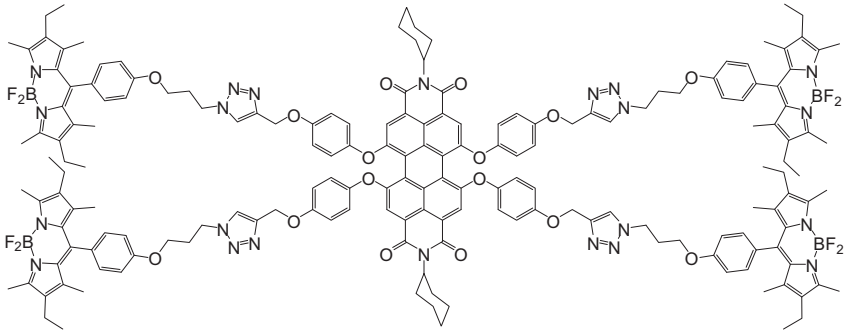

7

Fig. 7. Tetra-BODIPY–perylenediimide array.

phosphoresce or still undergo charge separation to give the charge-separated species before charge recombination.

A similar series of compounds has been prepared, which consists of one, two and four BODIPYs (one attached to each phenyl ring of the zinc-porphyrin) attached by amide linkers.[30] In the case of the two BODIPY array, the two donor units were attached in a trans-configuration. A fullerene terminating in an imidazole unit was then coordinated to the zinc centre (effectively forming a square-pyramidal zinc centre) to allow for electron transfer to occur. The larger number of BODIPY units increase the absorption peak corresponding to the BODIPY, effectively increasing the antenna effect of this array. A similar energy diagram to that shown in Fig. 6 was produced for this compound.

A simple BODIPY–fullerene dyad has also been shown to assume the triplet state by charge recombination.[31] In this array, singlet–singlet energy transfer occurs very rapidly from the BODIPY to the fullerene unit. The fullerene triplet state is then occupied by inter-system crossing. Due to the fullerene having a long triplet lifetime, triplet–triplet energy transfer occurs from the fullerene to the BODIPY, despite the higher thermodynamic position. This causes an enhanced triplet yield for the BODIPY, which is usually less than a few percent, to approximately 25%. The rate of energy transfer in this dyad is highly sensitive to the solvent system used, with electron transfer from the BODIPY onto the fullerene being quicker and the charge-transfer state being longer lived in a polar

red shifting the absorption and emission wavelengths of this unit, making it the acceptor. When excited at 501 nm (tetra-methyl BODIPY 'arm') and 572 nm (mono-styryl BODIPY 'arm'), emission is observed at 662 nm (central di-styryl BODIPY). This emission is also observed when the central BODIPY is excited directly. The efficiency of the energy transfer from both BODIPY 'arms' was calculated to be 99% in each case.

2.2. Through-bond energy-transfer cassettes

Förster energy transfer is the primary mechanism by which through-space energy transfer occurs. This is mainly governed by the spectral overlap of the donor fluorescence and the acceptor absorbance. However, if the donor and acceptor are joined by a conjugated system of multiple bonds, then through-bond energy transfer can occur. The conjugated system must be twisted or the whole molecule will act as one fluorophore. This mode of energy transfer does not follow the same rules as through-space energy transfer. Good spectral overlap is not required, meaning that an array with a large 'apparent Stokes' shift' can be produced.

Lindsey made the initial studies into the efficiency of through-bond energy transfer involving BODIPYs as donor units.[35] The main factors affecting through-bond energy transfer were proposed as being steric interaction, characteristics of the HOMO and LUMO and the site of attachment and type of linker between the donor and

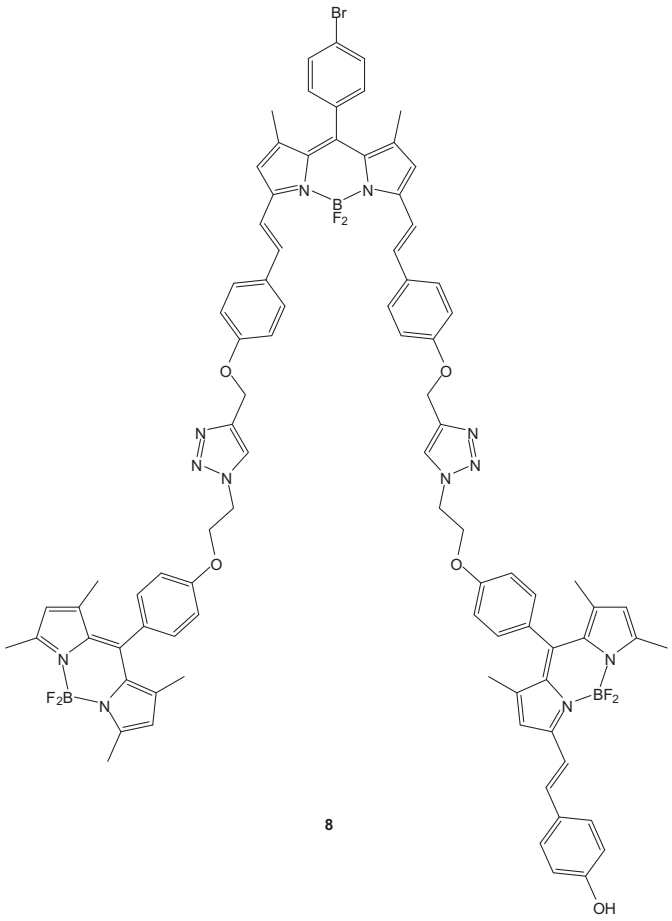

8

Fig. 8. Tri-BODIPY array.

acceptor. Increased rotational restriction was found to reduce both the rate and efficiency of energy transfer. Due to the energy transfer occurring along the conjugate system, through-bond energy transfer arrays have been described as molecular wires. Various BODIPY–porphyrin through-bond energy-transfer cassettes have been synthesised to investigate their energy-transfer properties.

The multi-porphyrin array depicted in **9** (Fig. 9) shows an example of a linear molecular wire.[36] As in the previous examples, the BODIPY is the donor component, while the free-base porphyrin is the acceptor component. Despite the distance between the donor and acceptor (90 Å in this case) efficient energy transfer still occurs (76%). This is an example of a through-bond energy transfer array in which the terminal porphyrin is the acceptor component, although there are BODIPY–porphyrin arrays in which the terminal unit is not the acceptor.

Molecular optoelectronic linear and T gates have been synthesised showing fluorescence on/off switching by oxidising or reducing an ancillary magnesium porphyrin (**10** and **11**) (Fig. 10).[37] When the magnesium centre is in its 2^+ state, fluorescence occurs at the free-base porphyrin by through-bond energy transfer from the BODIPY donor. When oxidised or reduced, fluorescence is quenched by intramolecular charge transfer. Energy transfer in these compounds was also very efficient, with values exceeding 80% for each array.

Multi-BODIPY–porphyrin arrays have also been synthesised, in order to increase the antenna effect of the BODIPY units.[38] One, two (**12** and **13**); Figs. 11 and 12, four and eight-BODIPY arrays have been prepared, each using the same BODIPY fluorophore. As seen for the multi-BODIPY–perylenediimide arrays, increasing the number of BODIPY units has little effect on the energy-transfer efficiency, but it does increase the amount of light absorbed by the compound at the BODIPY excitation wavelength. While the energy-transfer efficiency of the mono- and di-BODIPY arrays was almost quantitative, the eight-BODIPY array displayed an efficiency of between 80 and 90%. In each case, the BODIPY was attached to the porphyrin via a phenylethynyl linker. In this series of compounds, the eight-BODIPY array consists of a free-base porphyrin with two BODIPY units attached to each of the four phenyl rings in the same fashion as the array depicted in **13**. The four-BODIPY array is similar in that a BODIPY is linked to each of the four phenyl rings of the porphyrin. Interestingly, a dithiaporphyrin analogue of the four-BODIPY system showed poor electron transfer (~ 11%) when excited at 485 nm.[39]

Through-bond energy transfer arrays consisting of BODIPY donors and 21-thia- or 21-oxoporphyrins have been prepared in a similar fashion to those in the previous examples (**14** and **15**); Figs. 13 and 14.[40,41] For both of these porphyrin analogues, efficient energy transfer was observed, as the porphyrin emission was enhanced when the array was excited at 485 nm. These reported energy transfer arrays are interesting, but a direct comparison is difficult, as the orientations of the BODIPY units are different for each compound.

This highly efficient energy transfer from BODIPYs to porphyrins has been exploited for photocurrent generation.[42] In this system, a BODIPY was the terminal donor unit and was attached to a zinc porphyrin acceptor unit, which also acts as the electron donor in a similar way to that in previous examples. This donor/acceptor system was then coordinated to a tri-osmium–fullerene unit, which can act as both an electron acceptor and donor. Diazabicyclooctane (DABCO) was then used to tether these arrays together by coordinating to two of the zinc-porphyrins via their axial positions. This ensured a high surface coverage when binding to the

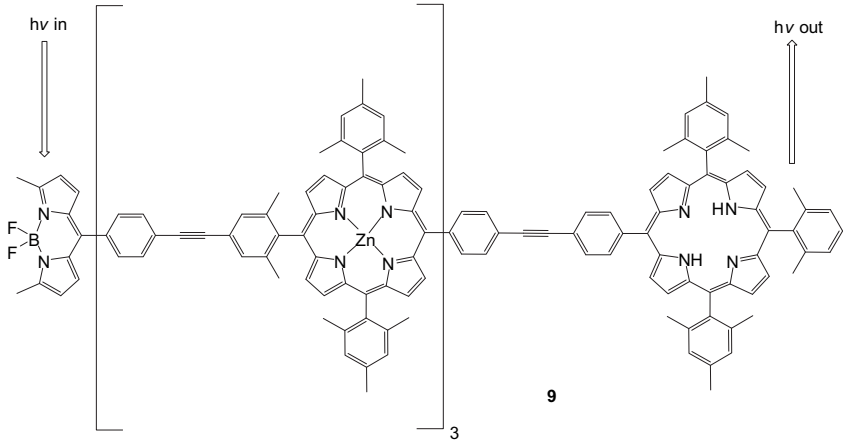

9

Fig. 9. BODIPY–tetraporphyrin array.

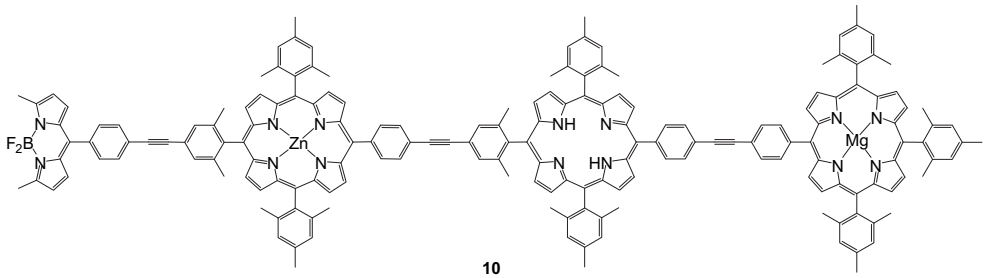

10

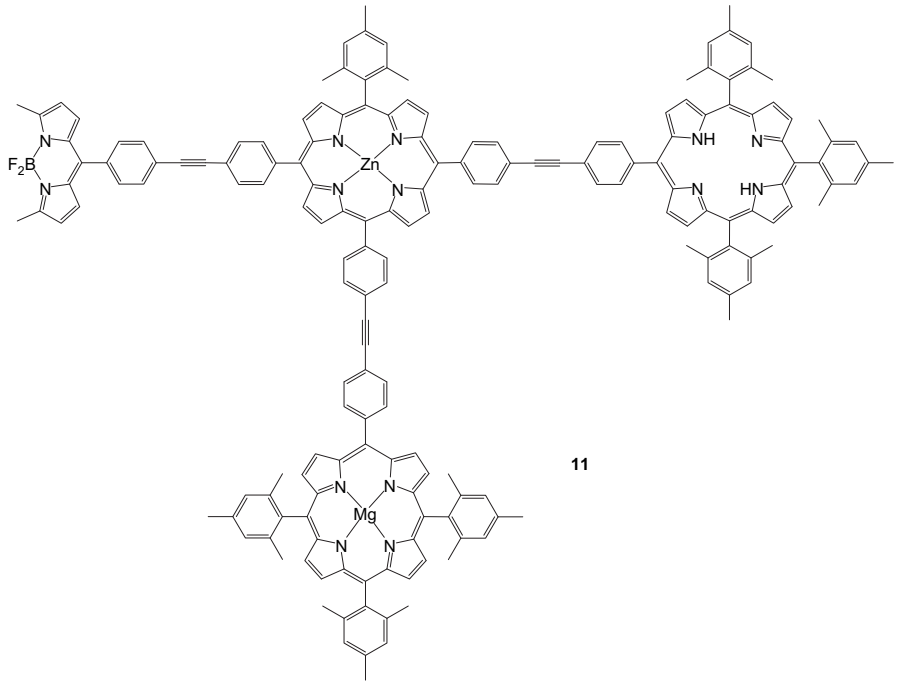

11

Fig. 10. BODIPY–porphyrin arrays.

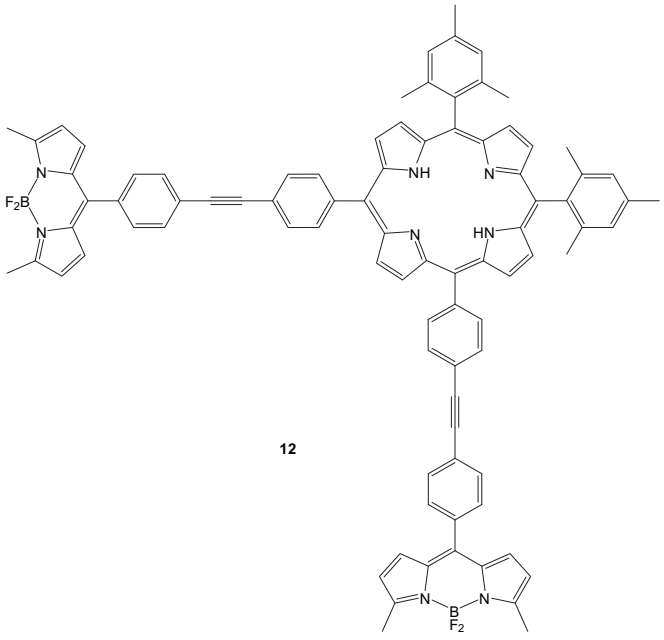

12

Fig. 11. Di-BODIPY–porphyrin array.

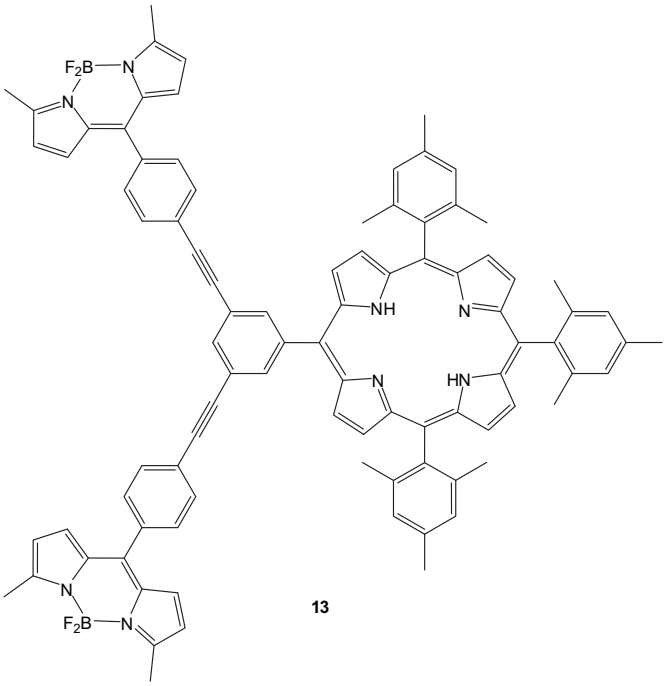

13

Fig. 12. Di-BODIPY–porphyrin array with BODIPY attachment at same phenyl ring.

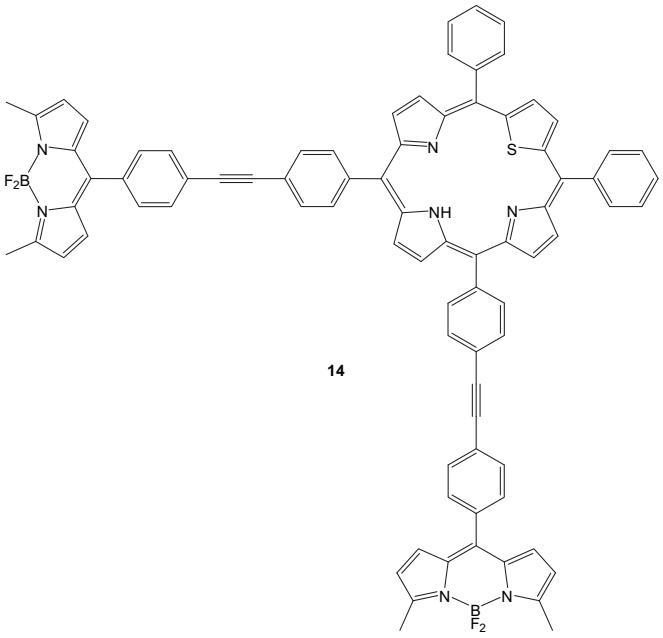

14

Fig. 13. Di-BODIPY–thioporphyrin array.

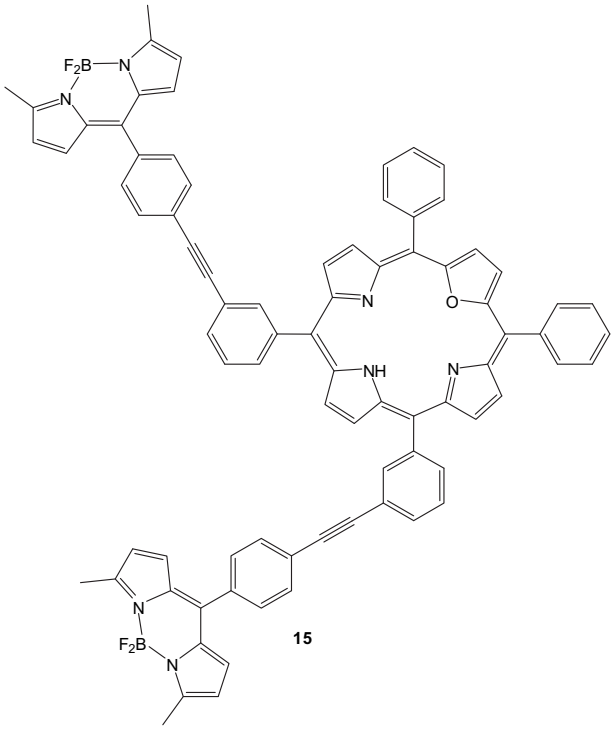

15

Fig. 14. Di-BODIPY–oxoporphyrin array.

electrode. The supramolecular array was then exposed to indium-tin oxide (ITO), which acted as one of the electrodes, the other being platinum. Photocurrent generation was initiated by excitation of the terminal BODIPY, which transferred its energy (through-bond) to the zinc porphyrin. Electron transfer then occurred from the zinc porphyrin to the fullerene, and subsequently from the fullerene to the ITO electrode. A sacrificial electron donor (ascorbic acid) was also used. The photocurrent generation efficiency was calculated as being 29%. This array was also found to be highly thermally and electrochemically stable.

While it has been shown that porphyrins are useful in constructing energy-transfer cassettes, this also provides a limitation on the types of arrays that can be formed. BODIPYs with attached metal complexes also provide an interesting class of compound that can be used as energy- and electron transfer arrays. Several polypyridine complexes of BODIPYs have been prepared and their energy- and electron-transfer properties have been investigated. Analogues of compound **16** (Fig. 15) have been prepared consisting of one or two BODIPY fluorophores, bis- or ter-pyridine ligands and various linker groups.[43–46] Metal(II) polypyridine complexes were chosen because of their intense and long-lived triplet metal-to-ligand change-transfer (MLCT) emission.

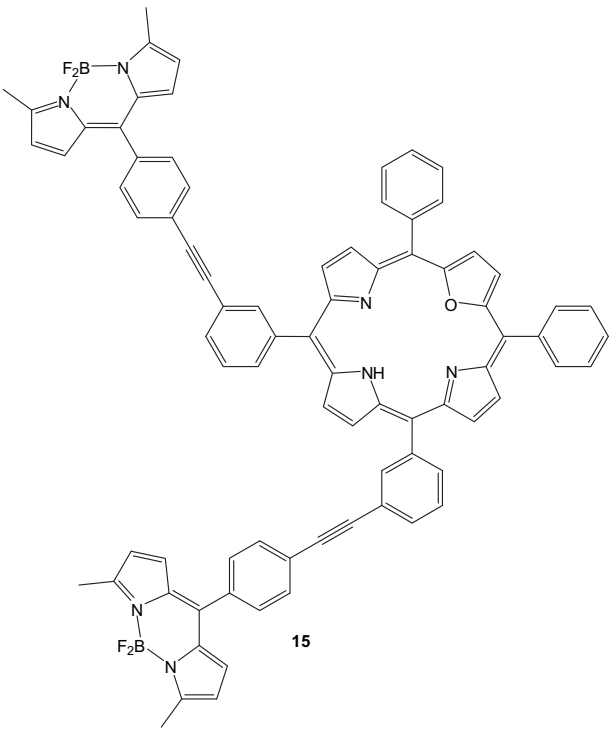

15

Fig. 15. BODIPY–bipyridyl–ruthenium complex.

For the ruthenium complexes at 77 K in a rigid matrix, the energy-transfer mechanism (Fig. 16) appears to proceed via initial excitation of the ruthenium–polypyridine complex to the ^{1}MLCT state, followed

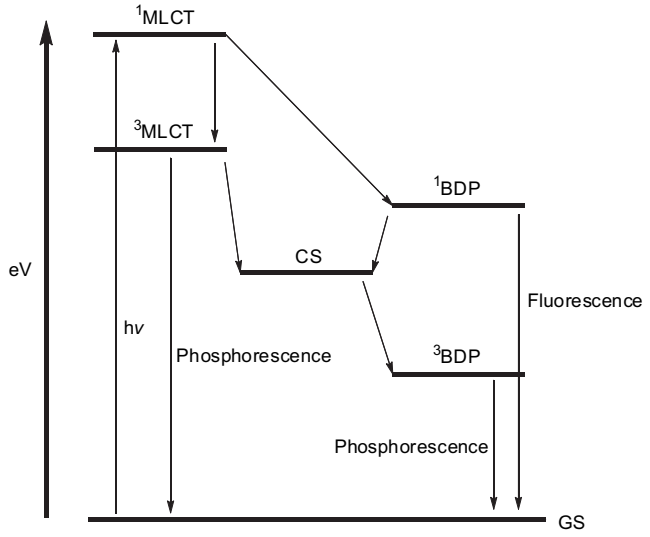

Fig. 16. Energy level diagram showing the various photochemical processes involved in the transfer of energy from the metal complex to the BODIPY.

by transfer of this energy to the ^{1}BDP state. This process can only proceed if the ^{1}MLCT and the ^{1}BDP energy levels are similar. The ^{3}BDP state can be reached via a charge-separated state. Phosphorescence can occur in some of the compounds and is attributed to the presence of the ruthenium, which promotes inter-system crossing from the ^{1}BDP state to the ^{3}BDP state by the 'heavy-atom effect'. The ^{3}BDP state can also be reached via energy transfer from the ^{3}MLCT state if the energy levels are close enough, as this process would be spin allowed.[47,48] Some BODIPY–ruthenium complexes have been prepared that have the effect of quenching fluorescence via energy transfer.[49] In the case of compounds **17** and **18** (Fig. 17), the ^{1}BDP state is quenched by energy transfer to the ruthenium centre with 93 and 73% efficiency, respectively. This transferred energy is then lost via electron transfer and singlet-to-triplet inter-system crossing.

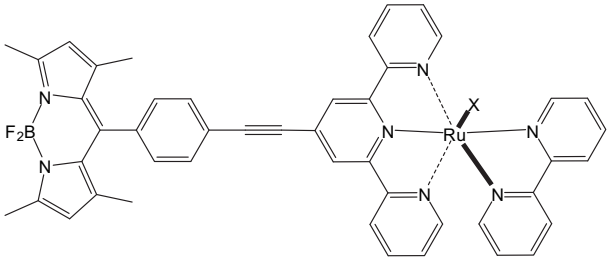

(**17**): X = Cl
(**18**): X = NCS

Fig. 17. BODIPY–oligopyridine–ruthenium complex.

Zinc–polypyridine complexes have been incorporated into energy transfer arrays in a similar fashion to the ruthenium complexes (**19** and **20**); Fig. 18.[50] In these complexes, the fluorescence of the BODIPY was quenched by intramolecular electron transfer. Extension of the distance between the terminal BODIPYs and the zinc centre, by incorporation of ethynyl groups, decreases the electronic coupling, but electron transfer still occurs to a large extent, resulting in fluorescence quenching. Analogous to the ruthenium complexes, the ^{3}BDP state is at a lower energy than the charge-separated state, but in this case charge recombination occurs preferentially over triplet state formation. It was proposed that charge recombination could be enhanced by preferential localisation of the positive charge at the *meso*-carbon in the BODIPY π-radical level or by quantum mechanical effects.

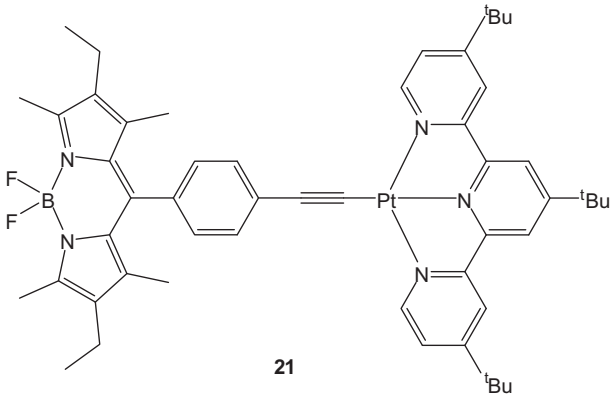

21

Fig. 19. BODIPY–terpyridine–platinum complex.

Platinum complexes analogous to **20** have been prepared and their energy transfer behaviour has been observed.[51,52] Compound **21** (Fig. 19) does not exhibit any fluorescence quenching of the BODIPY, compared to the zinc complex. However, luminescence from the ^{3}MLCT of the platinum centre is quenched by energy transfer to the ^{3}BDP state, both at 77 K and at room temperature. The heavy-metal centre also promotes inter-system crossing in the BODIPY and allows phosphorescence to occur.

Mono- and di-styryl (**22** and **23**) analogues of **21** have also been prepared as well as an array involving an ethynyl pyrene unit, which replaced the fluorines on the boron centre (**24**) (Fig. 20).[52] In each of these arrays, excitation to the ^{1}MLCT state leads to decay to the ^{3}MLCT state, instead of the ^{1}BDP state. In the **23** and **24** analogues, triplet–triplet energy transfer via a charge-separated state is almost quantitative. While still efficient in **22** (>90%), triplet–triplet energy transfer is less efficient, due to a shorter ^{3}MLCT lifetime. In **24**, through-space energy transfer occurs quantitatively from the pyrenyl moieties to the BODIPY. This means that the ^{3}BDP is being occupied by an electron from the charge-separated state (generated from the ^{3}MLCT), while the ^{1}BDP state is acting as an acceptor for energy from the pyrene units. When these compounds are held in a rigid matrix at 77 K, this charge-separated state does not appear to be the intermediate by which the energy from the ^{3}MLCT is transferred to the ^{3}BDP state. The most likely energy-transfer mechanism in this case would be through-bond energy transfer. Being held at 77 K also allows phosphorescence of **24** to be observed. It is assumed that phosphorescence occurs from **22** and **23**, but this is more difficult to detect, as it would emit in the IR region.

Due to their high stability and versatility, ferrocene derivatives have also been incorporated into electron-transfer systems involving BODIPYs. In the case of the styryl-ferrocenyl–BODIPY (**25**) (Fig. 21), it was found that the molecule underwent remarkable electro-

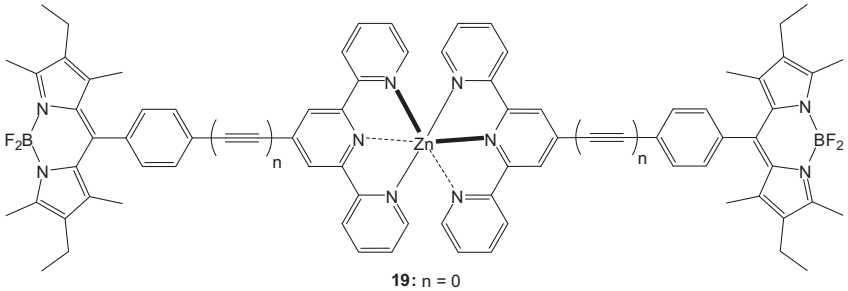

19: n = 0
20: n = 1

Fig. 18. BODIPY–terpyridine–zinc dimer.

chromism.[53] A clearly visible colour change occurred when the molecule went from its neutral to oxidised state (purple) and back again (blue). Compound **26** did not exhibit any fluorescence, due to electron transfer from the ferrocene to the BODIPY.[54] Electrochemical

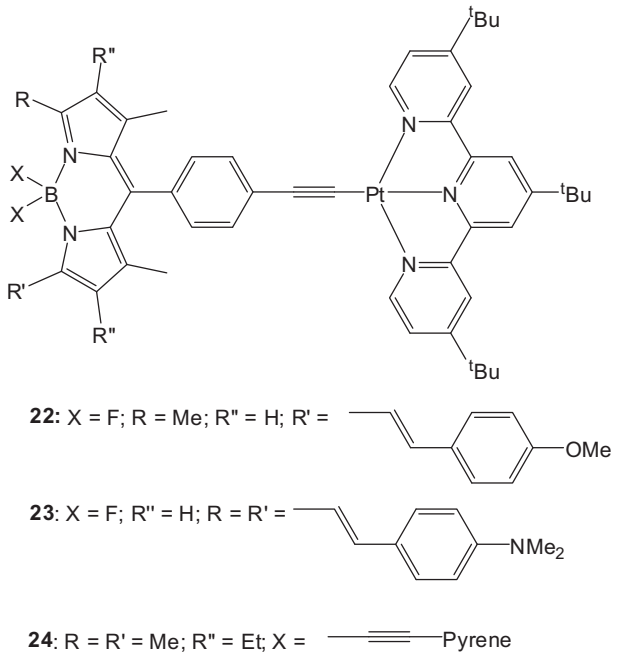

Fig. 20. BODIPY–terpyridine–platinum complexes with differing acceptor moieties.

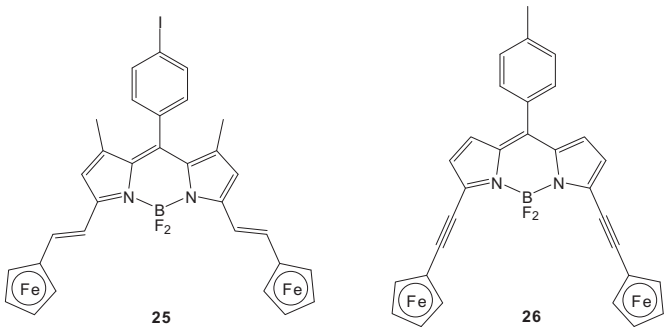

Fig. 21. BODIPY–ferrocene arrays.

studies showed that the ferrocene unit is difficult to oxidise, but the BODIPY unit is relatively easily reduced. A ferrocene moiety has also been used in the preparation of a ferrocene–BODIPY–fullerene triad.[55] This triad caused charge stabilisation, allowing electron transfer to occur readily. Excitation of the BODIPY causes abstraction of an electron from the ferrocene moiety, producing a BODIPY anion radical. A second electron transfer then occurs from the BODIPY onto the fullerene unit. Due to the distance between the cation and anion radicals, charge stabilisation is achieved.

While energy transfer arrays based on porphyrins and metal complexes display remarkable potential as molecular wires and fluorescent switches, the size of these molecules precludes much of their practical use for optoelectronic applications. It seems necessary, therefore, to prepare smaller cassettes via simpler synthetic routes. To this end, several BODIPYs bearing anthracene moieties have been prepared and their energy-transfer effects studied. Compound **27** (Fig. 22) has the anthracene unit attached directly to the 5-position of the BODIPY.[56] Despite the lack of methyl groups on the BODIPY core, the anthracene unit adopts a near-orthogonal geometry with respect to the BODIPY plane. This was also observed in the 1,3,5,7-tetramethyl analogue of the same BODIPY.[57] This BODIPY appears to undergo similar photochemical processes to those depicted in Fig. 16. The ^{1}BDP state can undergo charge separation with subsequent formation of the ^{3}ANT state. This ^{3}ANT state can then decay to the ^{3}BDP state. This energy transfer (which

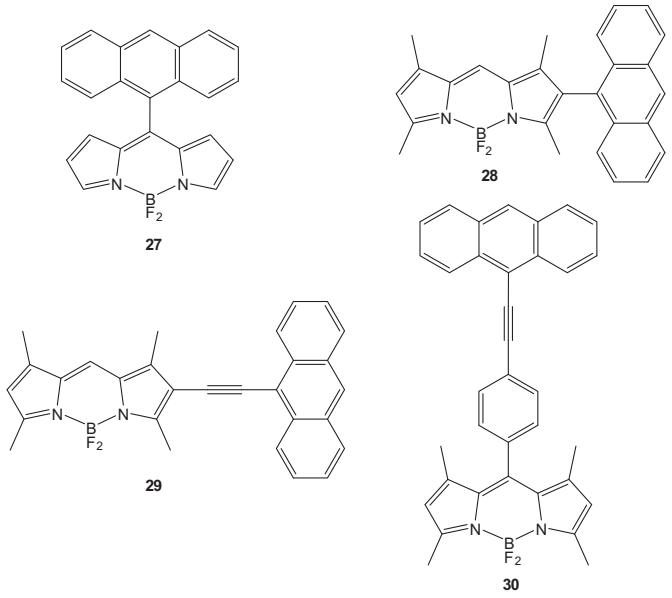

Fig. 22. BODIPY–anthracene arrays.

was susceptible to changes in temperature) does not occur to any great extent, and thus makes this particular compound unsuitable as an energy transfer array.

A series of anthracenyl–BODIPYs were synthesised to investigate the effects of donor–acceptor separation and attachment position on their energy-transfer properties.[58] It was shown that arrays analogous to compound **30** display energy transfer, but despite several acceptor BODIPY units being investigated, no correlation between the structure of the acceptor and the efficiency of energy transfer was observed. In arrays, such as **28** and **29**, much faster energy transfer was observed. Greater steric effects around the site of attachment to the BODIPY force the anthracenyl moiety out of the plane of the BODIPY. This, however, proved to be problematic, as the energy transfer was too fast to allow measurements of the exact rate to be determined, meaning that a relationship between energy transfer and donor–acceptor separation may exist, but cannot be measured. This may, however, imply that the orientation of the BODIPY has a greater effect on the energy transfer than the BODIPY substitution.

Replacement of the fluorine atoms on the boron provides another route towards the preparation of energy-transfer cassettes. Pyrene and perylene donors have been attached to the boron and efficient energy transfer occurred to the BODIPY acceptor; only emission from the BODIPY was observed.[59] A competing energy-transfer process takes place in compound **31** (Fig. 23) as energy

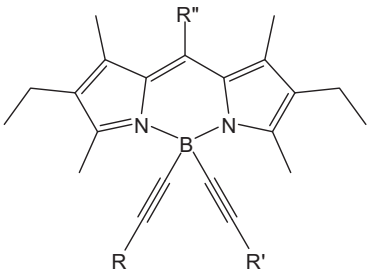

(**31**): R = R' = Pyrene; R" = Me
(**32**): R = Pyrene; R' = Perylene; R" = Me
(**33**): R = R' = Perylene; R" = Me
(**34**): R = R' = Pyrene; R" = 4-Pyridyl

Fig. 23. BODIPY arrays prepared by F-substitution.

absorbed by the pyrene unit can be transferred to the perylene unit with a similar efficiency as it is transferred to the BODIPY. In particular, compound **31** shows potential as a light harvester, due to strong absorptions in the UV region from the pyrene and perylene units. The energy-transfer properties of this type of array have been used to develop an orthogonal sensor.[60] Compound **33** displays efficient energy transfer from the pyrene units to the BODIPY, as expected. Exposure of compound **33** to protons switches on an intramolecular charge-transfer process, thus decreasing the fluorescence of the BODIPY. This also causes the absorption band of the BODIPY to undergo a red shift. As the absorption of the pyrene moieties is insensitive to cation coordination, the red shift in BODIPY absorption causes a decrease in the rate of through-space energy transfer, thus restoring some of the pyrene fluorescence. An additional aromatic unit was attached in compounds **32** and **34** in order to maximise its spectral coverage.

As an extension of this work, a BODIPY, which absorbs and emits in the red region was prepared and pyrene moieties attached to the boron in a similar fashion.[61] In each compound of the series **35**–**39** (Fig. 24), efficient energy transfer occurs from the aromatic moiety tethered to the boron and only emission from the BODIPY core is observed. The BODIPY itself emits at 750 nm, so there is a very large apparent Stokes' shift. Even in compound **39**, where two different donor groups are used, only emission from the BODIPY core is observed, indicating that, even if energy transfer occurs from one donor to the other, it is still then transferred to the BODIPY core. While it would appear that energy transfer in these compounds (*F*-substituted BODIPY arrays) would proceed via a Förster-type mechanism, poor alignment of the transition dipoles of the donors in relation to the acceptor (steric effects causing twisting of the donor units) minimises this mechanism and through-bond energy transfer is promoted by effective electronic coupling. It is, however, important to note that through-space energy transfer in these compounds is not eliminated, merely minimised in certain cases.

In an attempt to increase the potential for these types of molecules to be used as light harvesters in optoelectronic devices, analogues bearing three donor moieties attached to a terminal BODIPY acceptor have been synthesised (**40** and **41**); Fig. 25,[62–64] the aim of this being to maximise absorption in the UV region. This feature would allow these molecules to be used as light harvesters in dye-sensitised solar cells. It was proposed, based on the studies of these compounds, that the boron centre is the main bottleneck for through-bond electron exchange. This factor could prove to be invaluable in the design of new arrays, BODIPY or otherwise.

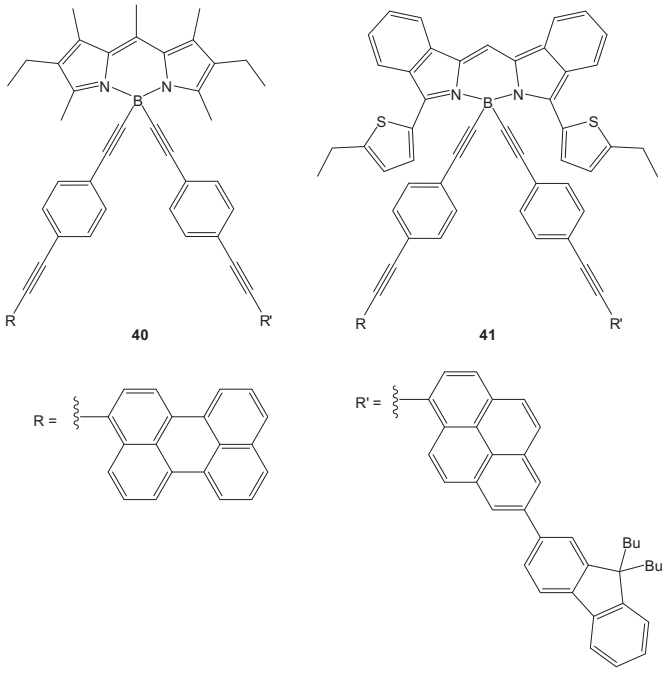

Fig. 25. BODIPY arrays bearing UV-absorbing donor groups.

While it has been shown that different chromophores can be used to maximise absorption in a particular region of the electromagnetic spectrum, no relationship between spacer length (between donor and acceptor) and energy transfer has been determined. Using the same F-substitution reaction as for the previous arrays, two BODIPYs have been attached to a terminal acceptor BODIPY via different-length aromatic linkers (**42**–**45**) (Fig. 26).[65] It was calculated that the length between the BODIPY

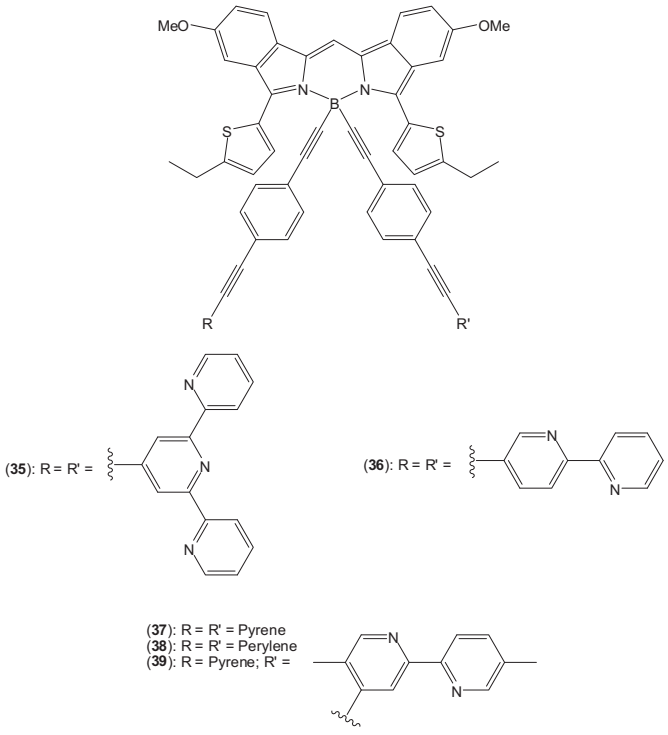

Fig. 24. BODIPY–oligopyridine arrays prepared by F-substitution.

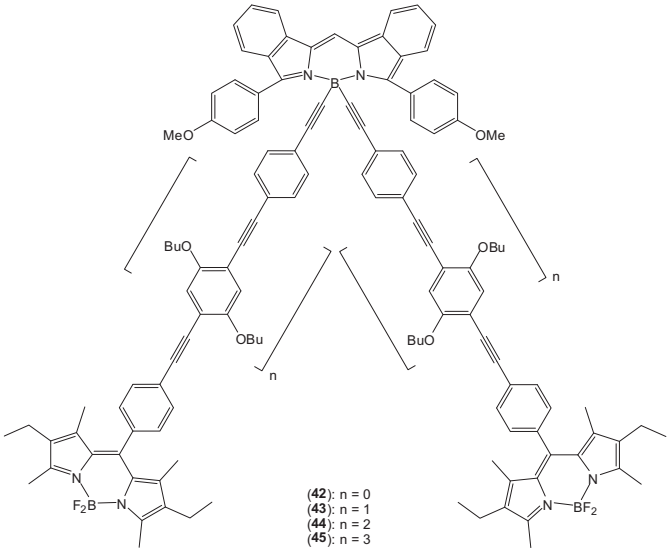

Fig. 26. BODIPY array exhibiting energy-transfer efficiencies dependent on spacer length.

acceptor and the donor was 18, 24, 31, and 38 Å for n=0, 1, 2 and 3, respectively. Due to the polyaromatic nature of the spacer groups, they absorb at increasingly red-shifted wavelengths as their length increases. This absorbed energy was shown to be almost quantitatively transferred to the terminal BODIPY acceptor. Energy transfer was shown to occur from the two BODIPY units to the terminal BODIPY acceptor, but with a decreasing rate as the spacer length increases. Similarly to compounds **40** and **41**, which contain three different donor units to maximise absorption in the UV region, compound **42** had the remaining BODIPY (donor) fluorine atoms replaced with pyrene units to achieve the same effect. Again, absorption in this region shows efficient energy transfer from the pyrene unit to the terminal BODIPY acceptor. In each of these compounds, emission from the donor BODIPY can still be observed to varying extents.

The original investigation into multi-BODIPY arrays was carried out by Burgess' group.[66] This involved the preparation of a series of bis-BODIPY arrays connected by different aromatic linker groups. In each case, efficient energy transfer was observed from the donor BODIPY to different acceptors via a through-bond mechanism. A small amount of donor fluorescence could still be observed for these arrays. This work was extended to prepare arrays consisting of two, three and four BODIPYs connected by a phenylethynyl linker.[67] The three- and four-BODIPY arrays were connected to the same single phenyl hub, as in **46** (Fig. 27). Efficient energy transfer occurs in each of the arrays from the BODIPY donor to the styryl-BODIPY acceptor. Emission from the donor is still observed, but is weaker than the emission from the acceptor (Φ_F=≤0.1 for donor emission, compared to Φ_F=0.27–0.42 for the acceptor from the various arrays). For these arrays, direct excitation of the acceptor moiety produced fluorescence quantum yields greater than those produced by energy transfer. The energy-transfer efficiency was calculated to be 99.5% and the increase in the number of BODIPY units provided the array with an increase in the antenna effect of the donor groups. It is interesting to note that despite the proximity of the BODIPY units in the four-BODIPY analogue, the donor units behaved as individual entities and there was no change in their individual photophysical characteristics.

Fluorene and truxene have also been used as bridging groups between different BODIPY units, due to their absorption in the UV region (Fig. 28).[68,69] In both the fluorene and truxene arrays, efficient energy transfer occurs from one BODIPY to the other. The fluorene was calculated to display almost quantitative energy transfer to the BODIPY, and energy transfer from the donor BODIPY to the acceptor BODIPY was calculated to have an efficiency of >90%. Efficient energy transfer from the truxene core to a donor group on one of the arms occurs, but there is little control over the acceptor to which it transfers. As the donor would have an absorption furthest into the blue region, and the acceptor furthest into the red region, with the donor/acceptor between the two, energy transfer can occur from the donor to both the donor/acceptor and the terminal acceptor, as well as from the donor/acceptor to the terminal acceptor. As energy transfer is very efficient (>90% for each process), but not quantitative, emission from the donor (weakest emission), donor/acceptor (intermediate emission) and terminal acceptor (most intense emission) is observed. For this array, through-bond energy transfer occurs from the truxene core to the BODIPY units and through-space energy transfer occurs from one BODIPY to another.

A simple energy-transfer system has been developed, which consists of one or two BODIPY acceptor units connected by a terphenyl donor unit.[70] This system has potential applications in photovoltaic solar cells, due to the terphenyl absorption in the UV region. A mono-BODIPY-terphenyl, which terminated in a hydroxyl group was also synthesised and was found to act as a pH sensor, with fluorescence quenching occurring at high pH values via a photoinduced electron transfer (PeT) mechanism. BODIPYs connected in other simple ways have also shown efficient energy-transfer properties. Simple multi-BODIPY arrays like **47** (Fig. 29) show efficient through-bond energy transfer from the three

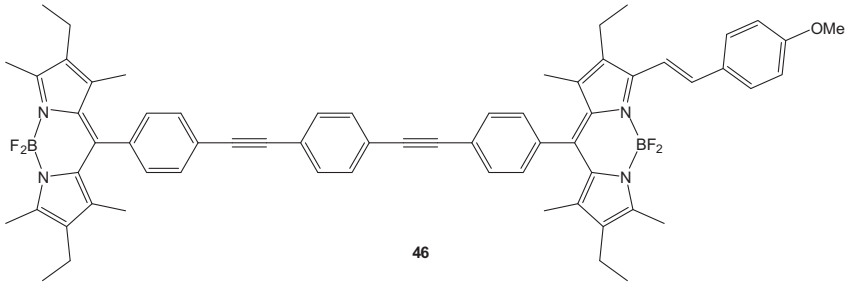

46

Fig. 27. Di-BODIPY array.

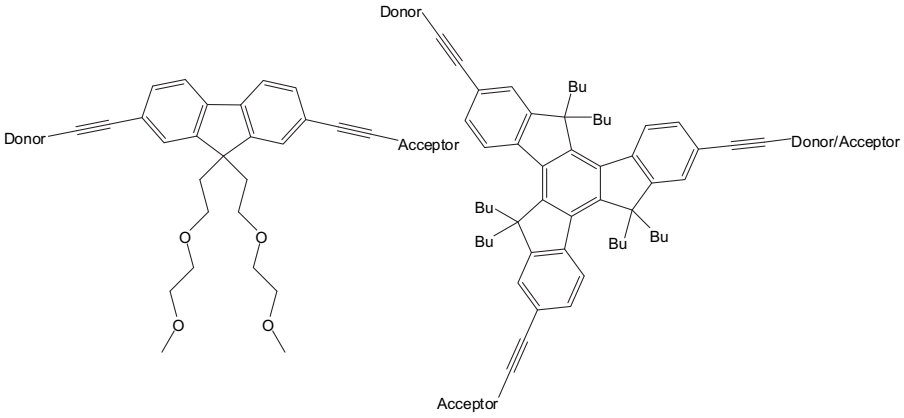

Fig. 28. Fluorene- and truxene-bridged arrays.

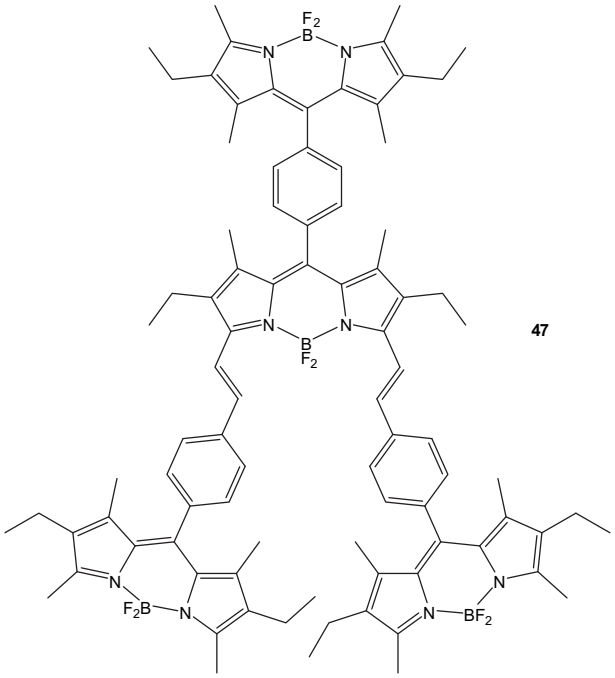

47

Fig. 29. Tetra-BODIPY array.

antenna donor BODIPYs onto the styryl-BODIPY, which acts as an acceptor, due to the styryl groups causing a significant red shift in the central BODIPY absorption and emission spectrum.[71] A series of one-, two- and three-BODIPY arrays were synthesised, with compound **47** being the in the latter category. In compound **47**, emission from the three donor BODIPYs is quenched completely while the acceptor BODIPY emission intensity is increased with increasing number of antenna BODIPY donors.

3. BODIPY-based energy transfer arrays as light-harvesting materials in electro-optic devices

The versatility of BODIPYs as components of energy-transfer cassettes is quite clear, but investigations into their practical use in electro-optic devices, particularly solar cells, is now also receiving attention. Photocurrent generation for practical use in solar cells can be achieved by employing the array as a sensitiser for titanium dioxide (dye-sensitised solar cells) or by the formation of bulk-heterojunction solar cells consisting of a donor/acceptor system bound between conducting surfaces (usually ITO and another metallic electrode).

3.1. Dye-sensitised solar cells

Dye-sensitised solar cells (DSSCs)[72,73] consist of a layer of dye trapped between a layer of titanium dioxide and an electrode. This is held between transparent electrodes (fluorinated tin oxide—FTO glass) to allow light absorption and to receive the photogenerated current. When the dye absorbs a photon, electron transfer from the dye to the titanium dioxide conduction band occurs. This electron then moves by diffusion to the anode. Due to the dye having lost an electron, an electrolyte solution is placed below the titanium dioxide layer, allowing regeneration of the dye ground state.

The binding of organic molecules to titanium dioxide is relatively straightforward (the carboxyl group binds readily) and thus BODIPYs have been the focus of some recent research into new dye-sensitised solar cells. For these devices to be efficient, the dye must absorb in a wide range throughout the electromagnetic spectrum, which would appear to be a problem for BODIPY dyes, given their relatively sharp absorption bands. However, as has been seen for some of the energy-transfer cassettes, various groups can be attached to the BODIPY to maximise the dye absorption and, thus, photocurrent generation. One of the earlier examples of BODIPYs as sensitisers involved a BODIPY with two triphenylamine groups attached via a styryl linker (**48**) (Fig. 30).[74] The styryl groups cause the BODIPY unit to absorb in the red region, while the triphenylamine unit absorbs in the blue and green regions. Given that the electron density of a BODIPY moves from the BODIPY core (HOMO) to the 5-phenyl group (LUMO) upon excitation, this allows a relatively simple site for charge injection. Cyclic voltammetry of **48** revealed that it possesses a LUMO of 3.517 eV, which allows thermodynamically favourable electron transfer into the titanium dioxide conduction band at 3.9 eV. Compound **48** was shown to have a photon-to-current efficiency of 22%.

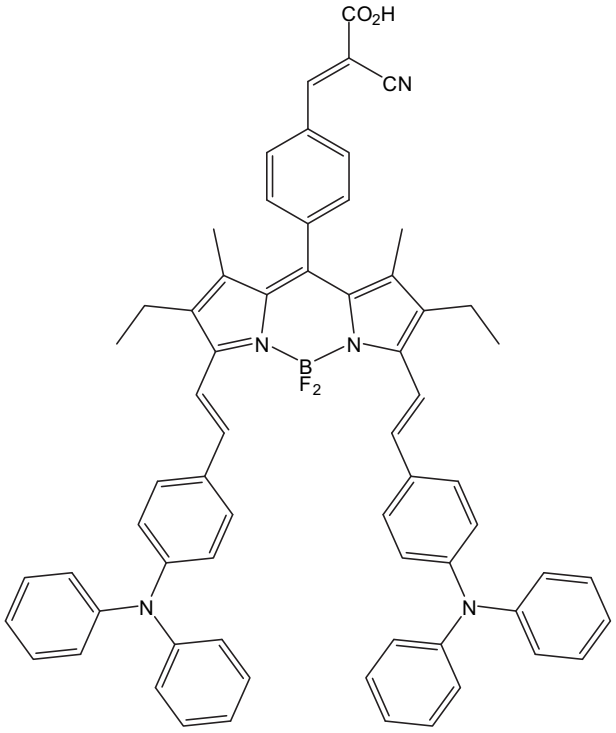

48

Fig. 30. Triphenylamine–BODIPY array for DSSCs.

The use of triarylamines as donor units for DSSCs has been extended by the same group to include different substituents on the unsubstituted aryl groups, different positions for binding to titanium dioxide and different substituents on the BODIPY core.[75] The different functional groups were used to shift the absorption maxima, as well as alter the oxidative and reductive potentials. It was observed that compound **49** (Fig. 31) gave the highest photon-to-current conversion efficiency of the three compounds synthesised. A higher conversion was observed in the blue region, rather than at the BODIPY absorption in the red region. Conversion efficiencies were lower for compounds **50** and **51**, indicating that the position of binding to titanium dioxide, as well as substituents on the BODIPY core, are important factors in the preparation of DSSCs. Compound **49** has the highest conversion efficiency of this series of compounds at 0.68%.

Because the synthetic route towards core BODIPYs is relatively straightforward, simple analogues of the same BODIPY core can be easily prepared and studied. This particular aspect of BODIPYs was

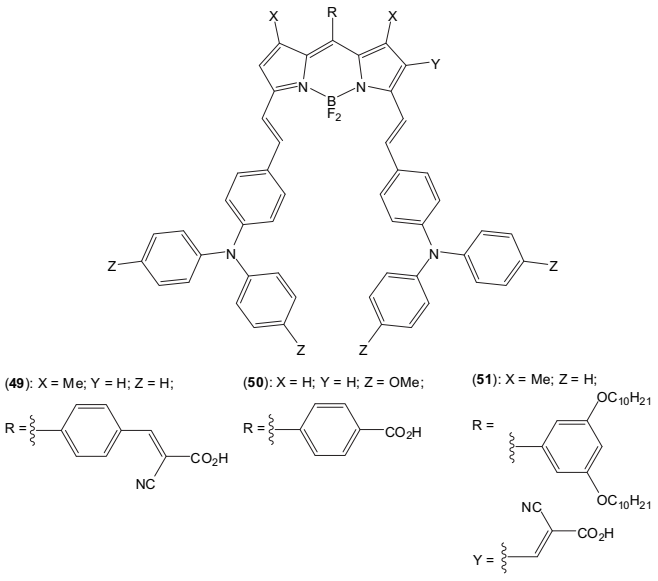

Fig. 31. Triphenylamine–BODIPY arrays for DSSCs bearing differing titanium dioxide-binding and UV-absorbing groups.

exploited to prepare three analogues of a BODIPY-containing poly (ethylene glycol) (PEG) arms for use in DSSCs.[76] The different BODIPY analogues absorbed at different wavelengths in the visible region (compounds **52**–**54**) (Fig. 32). The addition of one, then two, styryl groups causes a progressive red shift in the BODIPY absorption, while the increased number of aromatic groups causes an increase in the UV absorption. The PEG chains provide the molecules with enhanced film-forming properties. Photocurrent generation was measured for these compounds, with excitation from 400 to 725 nm. As expected, compound **52** displays photocurrent generation over the shortest region, due to the absorptions of the BODIPY in the UV and visible regions being closer together than those for **53** and **54**. Compound **54** displayed photocurrent generation over the entire region of the measured spectrum, due to its wider absorption profile. No photon-to-current efficiencies were reported for these compounds.

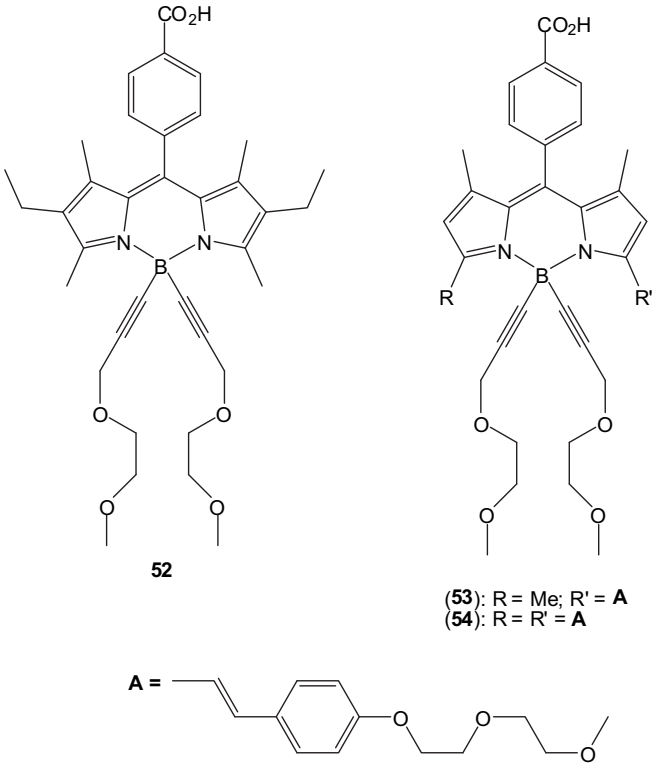

Fig. 32. BODIPYs for DSSCs with PEG arms to enhance film formation.

Energy transfer in through-bond BODIPY porphyrin arrays has been shown to be very efficient and this effect has already been exploited in a photocurrent-generation system.[42] This work has been extended to produce a BODIPY–porphyrin array bound to titanium dioxide for use in DSSCs (**55**) (Fig. 33).[77] A through-bond energy-transfer mechanism takes place to transfer energy from the BODIPY to the porphyrin and subsequent electron transfer occurs onto the titanium dioxide. While the zinc porphyrin absorbs strongly at ~440 nm and more weakly at ~640 nm, the BODIPY absorbs at ~520 nm, providing the array with three distinct absorption regions, which promotes photocurrent generation across a wide wavelength range. An analogue without the BODIPY donor was also synthesised, which showed a drop off in photocurrent generation around 500 nm, while the array containing the BODIPY (**55**) maintained photocurrent generation throughout the measured wavelengths (400–700 nm). Peak photocurrent generation was centred on the strong zinc porphyrin absorption around 440 nm, with two smaller peaks at the absorptions of the BODIPY (~520 nm) and the weaker porphyrin absorption (~660 nm). This array exhibited a photon-to-current efficiency of 1.55%.

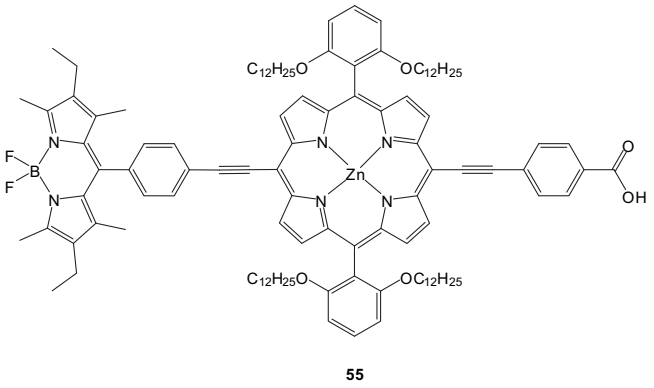

Fig. 33. BODIPY–porphyrin array for DSSCs.

While BODIPYs display efficient energy transfer, dipyrrin–metal complexes also exhibit strong absorptions in the UV and blue-green region of the visible spectrum. Although dipyrrin–metal complexes have not yet been incorporated into DSSCs, their binding to titanium dioxide has recently been studied.[78] Rhodium, palladium and ruthenium complexes of 5-(4-carboxy)phenyl-dipyrromethene were synthesised and were shown to bind to titanium dioxide and their absorption profiles were measured. However, no photocurrent-generation experiments were reported for these compounds.

3.2. Bulk-heterojunction solar cells

Bulk-heterojunction solar cells (BHJs) consist of a charge donor and acceptor dispersed throughout a polymer matrix. Initially, the donor and acceptor were separated in a bilayer (bilayer-heterojunction solar cells[79,80]), but charge transfer was found to be inefficient. By dispersion throughout a polymer matrix, more interfacial contact between the donor and acceptor occurs and charge transfer is more efficient.[81] Besides the increased efficiency of BHJs, their other major advantage is that, because they are a dispersed mixture of donor and acceptor, they can be fabricated by relatively simple solution-based processes, thus decreasing their

production costs. Fullerene analogues have been the focus of interest in the development of BHJs, due to their low LUMO energy level promoting efficient photoinduced charge transfer, their highly delocalised π-system conferring stability on any charge-separated state and spherical geometry leading to isotropic electron transport through the 3D system.[81,82] However, aromatic polymers have been the main avenue of research in the development of BHJs, due to their ability to act as molecular wires, their low band gap and their high electron-hole mobility. Oligothiophenes in particular have attracted interest, but their synthesis, purification and electronic properties have caused some degree of difficulty in the preparation of BHJ devices.[83–85]

The initial investigation of the potential for BODIPYs as dyes for BHJs was carried out using three commercially available BODIPY dyes to dope an acrylate polymer and their effects as solar concentrators were measured.[86] Fig. 34 shows the three different BODIPY dyes (shown as triangles, squares and circles) dispersed throughout the acrylate polymer. The first dye (A—BODIPY 494/505) absorbs the incident sunlight and then transfers the energy by FRET to the next dye (B—BODIPY 535/558), which subsequently transfers it to the final dye (C—BODIPY 564–591). It was found that 75% of the light emitted from dye C is trapped within the plate and guided to the photovoltaic cell by internal reflection. The white scattering surface reflected unabsorbed light from the first pass through back into the plate. While efficient energy transfer was observed for this system, no photocurrent generation results were reported.

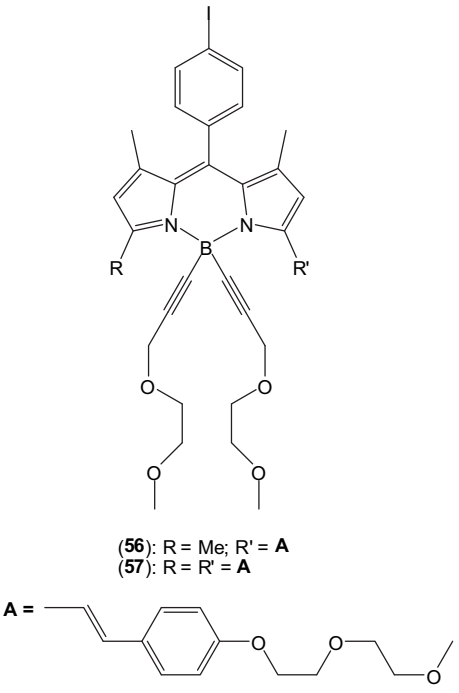

Fig. 34. BODIPY for BHJs with PEG arms to enhance film formation.

Analogues of compounds **53** and **54** were prepared for use in BHJs that comprised identical molecules in which the carboxyl group had been replaced with an iodo group (compounds **56** and **57**) (Fig. 34).[87] Compound **56** was found to have an excitation of 572 nm, while **57** had an excitation of 646 nm. When cast as thin films on ITO glass and bound in PEDOT-PSS (polymer support), a slight red shift in the absorption maxima was observed. BHJs of these compounds were produced by spin coating a mixture of BODIPY with [6,6]-phenyl-C_{61}-butyric acid methyl ester (PCBM) in a 1:2 weight ratio onto ITO glass treated with a 40 nm thick layer of PEDOT-PSS. These cells showed distinct photocurrent generation around the major absorption peaks. An impressive power conversion efficiency[88–90] of 1.34% was calculated for these cells. The power conversion efficiency of these compounds was increased by using mixtures of both **56** and **57** with PCBM in PEDOT-PSS, and coating ITO glass with the mixture.[91] The combination of the two different BODIPY dyes allows photons to be absorbed over a broader spectral range. The power conversion efficiency for these mixtures was calculated to be 1.70%.

Due to the interest in oligothiophenes as donors in BHJs, a bis (thiophene) analogue of compound **57** has recently been prepared that combines the light-harvesting properties of the di-styryl-BODIPY with the electron-hole transport properties of an oligothiophene (**58**).[92] Compound **58** (Fig. 35) displays strong absorption between 300 and 700 nm with major peaks for the BODIPY chromophore and strong absorption for the aromatic groups in the UV region. As predicted, the photocurrent-generation profile matches the absorption profile and the power conversion efficiency was calculated as being 2.20% when mixed with PCBM in a PEDOT-PSS matrix.

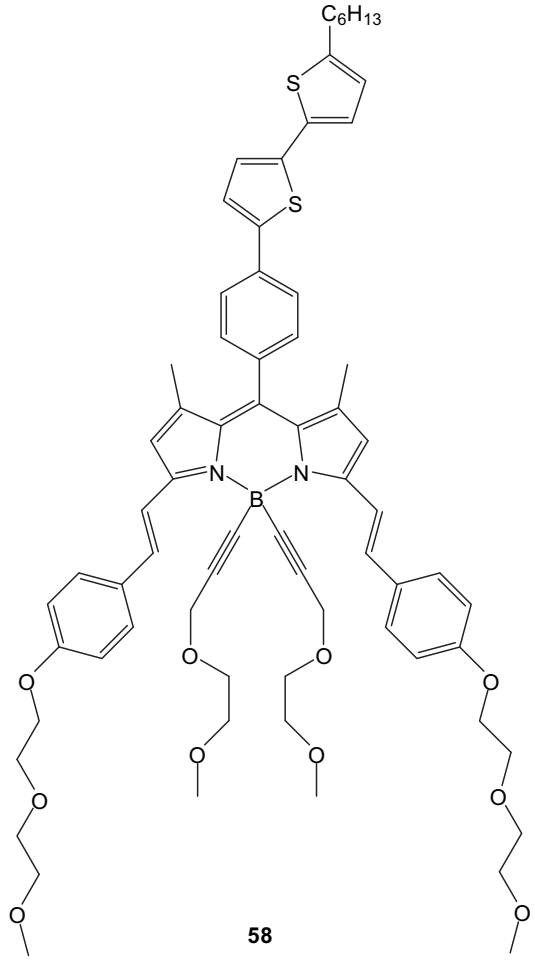

Fig. 35. BODIPY–thiophene array for BHJs.

4. BODIPYs as laser dyes

Several BODIPY derivatives have been shown to exhibit laser activity. Some of the BODIPY derivatives studied exhibit relative efficiencies above that of rhodamine 6G (against which the laser activity of this series of BODIPY dyes was compared, with rhodamine 6G having a relative efficiency (RE) of 100).[93,94] Drexhage described a simple rule governing the laser activity of fluorescent dyes, which relies on π-electron distribution.[95] The rule states that: 'in a dye where the π-electrons of the chromophore can make a loop when

oscillating between the end groups, the triplet yield will be higher than in a related compound where this loop is blocked. It may be said that the circulating electrons create an orbital magnetic moment, which couples with the spin of the electron. This increased spin-orbit coupling then enhances the rate of inter-system crossing, thus giving rise to a higher triplet yield.' BODIPYs are, therefore, ideal candidates for laser dyes, due to their sharp emission profiles and low rate of inter-system crossing, which is kept low by the lack of conjugation through the boron atom.

In one of the initial studies of BODIPYs as laser dyes, Boyer et al. synthesised 28 different BODIPY derivatives and their photophysical behaviour, including relative laser efficiency, was observed.[96,97] The BODIPYs synthesised were designed to cover a wide range of relatively simple functional groups in order to observe their effects on the lasing properties. Different types and numbers of alkyl substituents as well as rigid cyclic motifs, aromatic units and polar groups were attached to the BODIPY core and a wide range of laser efficiencies was observed (Fig. 36). Several of the BODIPYs studied have since been commercialised.

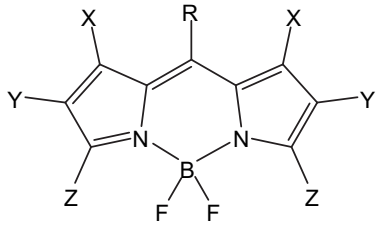

Fig. 36. Core BODIPY structure for investigation into laser activity of different BODIPY derivatives.

For the initial sub-series (seven compounds), an investigation into the effect of different short alkyl groups on the laser activity was carried out. A gradual red shift was observed with increasing alkyl substitution, with tertiary-butyl groups providing the largest shift (commercial BODIPY PM 597). A red shift of ~30 nm was observed for all the BODIPYs studied in going from their emission wavelength to their lasing wavelength. This sub-series showed an odd/even effect based on the number of alkyl groups present on the BODIPY core with regard to their relative laser efficiency. BODIPYs containing an odd number of carbon atoms possessed lower relative efficiencies than those with even numbers of carbon atoms. The even-number derivatives had relative efficiencies of at least 100, with PM 597 having a relative efficiency of 110. Over the whole series of 28 compounds, no clear relationship between absorption wavelengths, extinction coefficient and fluorescence quantum yield and laser activity was established, but replacing the *meso*-alkyl group with a hydrogen atom caused a marked decrease in laser activity. Distortion of the planarity of the BODIPY core caused by strong steric interactions between alkyl units caused a total loss of laser activity. Phenyl groups attached to the pyrrolic positions of the BODIPY also caused low lasing activity.

This initial research has, naturally, led to various groups preparing other BODIPY derivatives in order to investigate the laser properties of the resulting dyes. Mono-amino and acetamido (**59** and **60**; Fig. 37) derivatives of a BODIPY dye were synthesised and

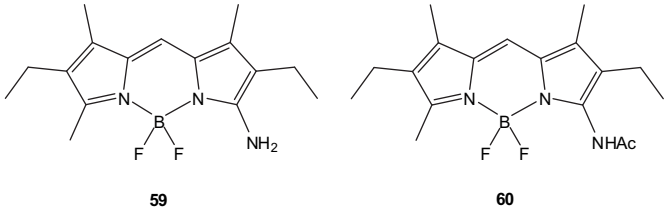

Fig. 37. BODIPY laser dyes.

remarkably different laser properties were observed.[98] The acetamido derivative displayed slightly red-shifted absorption and emission, compared to the amino derivative, but similar fluorescence quantum yields were observed. However, **60** displayed a laser efficiency of 48%, while **59** did not exhibit any laser emission. This lack of laser emission was not attributed to aggregation in solution, but could be due to the delocalised lone pair of the amino group attached directly to the BODIPY core.

In order to produce laser dyes with red-shifted emissions, BODIPYs with extended conjugated π-systems have been prepared (**61**–**63**; Fig. 38).[99] The two phenyl groups cause a red shift in the absorption (~50 nm) and emission (~80–90 nm) of the dyes with respect to the unsubstituted dye, as well as causing much wider Stokes' shifts than normally expected for BODIPY dyes. Despite the lack of alkyl groups restricting the rotation of the *meso*-phenyl ring, the fluorescence quantum yields are moderate (Φ_F=0.41–0.62). This was attributed to the efficient coupling between the electron clouds of the BODIPY core and the phenyl rings causing a restriction in their rotation. Compound **61** was found to possess the highest laser efficiency in several solvents, with acetone and ethyl acetate being the most suitable. Excitation at 532 nm caused a laser efficiency (in EtOAc and acetone) of 14%, while excitation at 568 nm increased this to 20%. This is likely due to the 568 nm excitation being closer to the three-BODIPY dye absorption maxima. Compound **62** displayed moderate laser efficiency in methanol with efficiencies of 11% and 17% for excitation at 532 and 568 nm, respectively. Compound **63** displayed the weakest laser efficiency of 5 and 11% in ethanol with excitation at 532 and 568 nm, respectively. Each of the BODIPY dyes studied appears to be photostable under laser pumping.

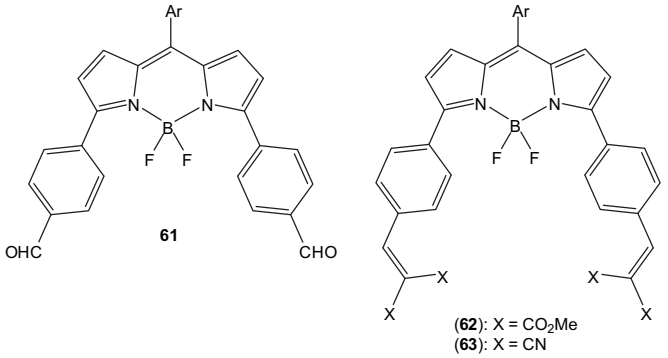

Fig. 38. BODIPY laser dyes with red-shifted absorption and emission.

This method of red shifting BODIPY emissions for use as laser dyes has been extended to include styryl groups and polyphenylene derivatives.[100] Compound **64** (Fig. 39) has the highest laser efficiency of this series (30% in THF) with compound **66** being similar (29% in THF). Despite having a similar core structure to **64**, compound **65** has a lower efficiency of 23% in THF. Compound **67** has the lowest efficiency of the series at 19% in THF, indicating that the trifluoromethyl units have the effect of increasing the laser efficiency of BODIPYs when attached to the styryl units.

4.1. Laser activity of dye-doped polymeric matrices based on commercial BODIPY derivatives

Commercial BODIPY dyes PM 567 and PM 597 (Fig. 40), have been used to dope linear and crosslinked fluorinated polymers.[101,102] An initial investigation into the effect that increasing crosslinking in dye-doped fluorinated co-polymers has on the lasing behaviour of the dye revealed a clear relationship between laser efficiency and stability of PM 567 and degree of crosslinking. The co-polymer host was a 2,2,2-trifluoromethyl methacrylate (TFMA)/

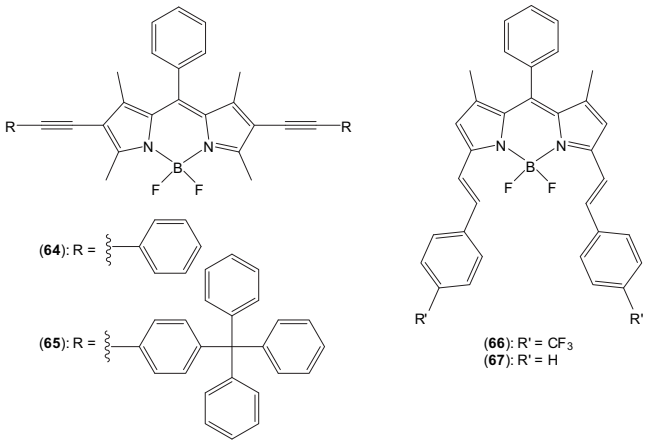

Fig. 39. BODIPY laser dyes with extended π-conjugation.

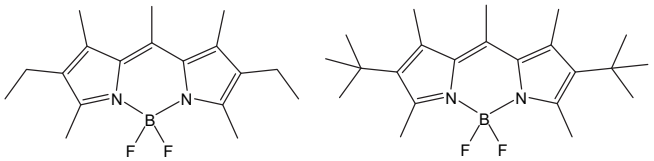

Fig. 40. Commercial BODIPY dyes PM 567 and PM 597.

ethylene glycol dimethacrylate (EGDMA) mixture with increasing proportions of EGDMA promoting increased crosslinking. A 99:1 TFMA/EGDMA mixture exhibited a laser efficiency of 4% and a stability of 15% after only 10,000 pulses (each stability of this series of TFMA/EGDMA co-polymers was measured after 5000 and 10,000 pulses; less than the usual 50,000 and 100,000 pulses). By increasing the amount of EGDMA to 2%, the laser efficiency was increased to 7% and the stability to 40%. The co-polymer containing 10% EGDMA was found to promote the highest efficiency and stability (18 and 55%, respectively) with further increases in the amount of EGDMA used causing a gradual decrease in both the efficiency and stability (80:20 TFMA/EGDMA having an efficiency of 14% and a stability of only 12%).

In an investigation into the effect of increasing the fluorine content of the co-polymer host on the lasing behaviour of the dye dopant, each of the polymers prepared was a methyl methacrylate (MMA) co-polymer using TFMA, 2,2,3,3,3-pentafluoropropyl methacrylate (PFMA) or 2,2,3,3,4,4,4-heptafluorobutyl methacrylate (HFMA) as the fluorinated monomers for linear polymers. The crosslinked co-polymers were prepared using MMA and EGDMA, pentaerythritol triacrylate (PETA) or pentaerythritol tetraacrylate (PETRA). Each co-polymer was prepared using two or three different proportions of monomers other than the EGDMA co-polymer, which was only prepared using MMA/EGDMA 80:20. PM 597 was only bound into linear co-polymers, while PM 567 was bound into both linear and crosslinked co-polymers.

In the series of linear co-polymers, PM 567 was shown to have the highest laser efficiency when bound in MMA/TFMA 70:30. This dye-doped polymer displayed a laser efficiency of 35%, but displayed a poor laser stability. The laser output intensity of this dye-doped polymer decreased to 26% after 100,000 pump pulses at the same position of the sample at 10 Hz. This decreased to 0% when pumped at 30 Hz. When PM 567 was bound in MMA/TFMA 50:50, the laser stability was reduced to 0% when pulsed at 10 Hz, with a very rapid drop in laser output by 92% after only 40,000 pulses. By switching to a monomer containing a higher weight percentage of fluorine atoms, the laser efficiency was slightly reduced, but the laser stability was dramatically increased. A mixture of MMA/PFMA 70:30 was found to give the best stability of 181% when pulsed at 10 Hz and 56% when pulsed at 30 Hz. The laser efficiency of this mixture was 22% which, although lower than the MMA/TFMA mixtures, is still moderate. By reducing the weight ratio of PFMA to 10%, a marginal increase in laser efficiency was observed (22–23%), but a decrease in laser stability was also seen (105% at 10 Hz, 0% at 30 Hz). This shows that the amount of fluorine attached to the co-monomer has a pronounced effect on the laser efficiency and stability. Contrary to the increase in laser stability caused by changing from TFMA to PFMA, the transition from PFMA to HFMA actually causes a reduction in laser stability, along with a slight increase in laser efficiency. An MMA/HFMA 70:30 mixture showed a laser efficiency of 24% and a laser stability of 115% (10 Hz) and 31% (30 Hz). The reported efficiencies of over 100% are due to an actual increase in laser output with increased number of pulses. No non-speculative explanation of this effect in BODIPYs has thus far been reported but it is assumed that it is due to multiple factors.

PFMA was chosen as one of the co-monomers for the crosslinked polymers, due to its moderate laser efficiency and high laser stability. The series of co-monomer mixtures for the crosslinked polymers was designed to investigate the effect that increased crosslinking had on the laser properties of PM 567. Similar laser efficiencies and emission wavelengths were observed for the crosslinked polymers, although the polymer mixtures containing PETA had slightly higher laser efficiencies. Laser stabilities are increased when going from mixtures containing 10% PETA to 20%, as well as from 10% PETRA to 20%, indicating a positive relationship between the degree of crosslinking and laser stability up to a certain point. Further increases were shown to be detrimental.

The investigations of the laser properties of PM 597 were carried out using linear co-polymer mixtures of increasing fluorine weight percentage and crosslinking co-polymers with an increasing degree of crosslinking. The linear co-polymers were prepared from 70:30 mixtures of MMA with TFMA, PFMA and HFMA and a dramatic increase in laser stability was observed, compared to PM 567. When bound in a mixture of MMA/HFMA (70:30), PM 597 showed the highest laser stability of all the series studied of 159% (10 Hz) and 105% (30 Hz) even after 500,000 pulses. This mixture also displayed a laser efficiency of 36%, equal to, or higher than, all the PM 567-doped co-polymers. The highest laser efficiency was observed for PM 597 in the crosslinked co-polymer PFMA/PETA 80:20 (42%), which also displayed an impressive laser stability [94.8% (10 Hz) and 59% (30 Hz) after 250,000 pulses]. While PM 567 displayed higher laser stability in the crosslinked co-polymers, PM 597 displayed much higher stability in the linear co-polymers. The loss of laser activity seen upon repeated pump pulsing is attributed to a build-up of heat in the polymer, which is more marked when pumped at a faster rate.

The impressive laser properties of PM 567 were also observed in silica aerogels with fluorinated co-polymers.[103] The co-polymers were 70:30 mixtures of MMA with TFMA, PFMA or HFMA with PM 567 dissolved in the co-monomer mixture, which was then incorporated into a silica aerogel by adding a silica gel monolith to the solution in order for polymerisation to occur within the aerogel. The MMA/TFMA aerogel produced a laser efficiency of 27% (lower than PM 567 in the co-polymer alone—35%) and a laser stability of 104% (10 Hz) and 38% (30 Hz), which is a significant increase over the stability of PM 567 dissolved in the co-polymer mixture alone [26% (10 Hz) and 0% (30 Hz)]. The MMA/PFMA aerogel caused an increase in the laser efficiency, when compared to the free co-polymer mixture (from 22 to 32%), as well as a decrease in the laser stability at 10 Hz (from 181 to 109%), but an increase in the stability at 30 Hz (from 56 to 105%). A similar effect was observed for the MMA/HFMA aerogel. While the effect of incorporating these dye-doped co-polymers into silica aerogels on the PM 567 laser efficiency appears to be unpredictable without further study, it is clear that it causes a significant increase in laser stability when pulsed at 30 Hz.

PM 567 has also been incorporated into a non-fluorinated co-polymer (1:1 MMA/HEMA) including a tetraethoxysilane (TEOS) inorganic component to investigate if BODIPY laser dyes could be used in organic–inorganic hybrid materials.[104] TEOS was added to the co-monomer/BODIPY mixture before polymerisation at 5, 10 and 15% proportions and a significant change in the laser stability was observed. The laser efficiency remained relatively unaffected (22, 20 and 24% for 5, 10 and 15% TEOS, respectively). When only 5% TEOS is used, thermal dissipation through the polymer matrix is increased, causing an increase in laser stability of the dye (69% after 60,000 pulses at 10 Hz). However, further increase in the amount of TEOS used causes a dramatic reduction in laser stability with 10% TEOS reducing the stability to 69% after only 7000 pulses and 15% TEOS reducing it even further to 69% after only 1800 pulses. While the addition of increasing amounts of TEOS causes a dramatic reduction in laser stability, it remains higher than the 1:1 MMA/HEMA mixture without any TEOS.[105–108]

An analogue of PM 567 has been prepared that possesses a styryl group (**68**) (Fig. 41) in order to produce a bathochromic shift in the absorption, emission and lasing wavelength.[109] The laser efficiency was determined to be as high as 18%, but varied depending on the solvent used. This styryl-BODIPY (**68**) was also bound in a polymer matrix and laser activity was still observed. Ethyl acetate was found to produce the highest laser efficiencies, so poly(methyl methacrylate) (PMMA) polymers were chosen, as MMA mimics the ethyl acetate solvent. Both linear and crosslinked polymers were studied, with linear polymers of two different molar proportions being prepared. Linear co-polymers MMA/TFMA 9:1 and 5:5 produced the highest laser efficiencies (18 and 16%, respectively), with crosslinked MMA/EGDMA 3:2 showing the lowest (6%). PMMA showed a laser efficiency of 10%, indicating that linear polymers allow the dyes to lase more efficiently than crosslinked polymers. By suspending the dyes in a solid polymer matrix, a slight red shift (~5 nm) was observed for the emission spectrum.

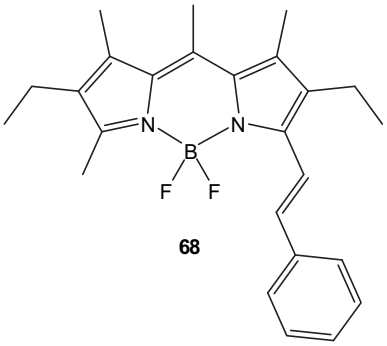

68

Fig. 41. Mono-styryl BODIPY dye.

Compounds **69**–**72** (Fig. 42) were designed to act as dopants for polymers (**69** and **70**) and as co-monomers for polymers (**71** and **72**).[110] The laser efficiency of compounds **69** and **71** was determined in several solvents and was most intense in ethanol (58 and 54%, respectively). They were then made up into solid solutions in PMMA and their laser efficiency and stability were determined. Compound **69** exhibited a laser efficiency of 27%, while the diacetyl analogue (**71**) had a laser efficiency of 33%. Compound **71** was determined to have a higher laser stability than **69** of 53%, compared to 35%, respectively. When used as co-monomers (**70** and **72**), the laser efficiency remains at a similar level (28 and 37%, respectively), but the laser stability increases significantly, [from 35 to 52% (**69** to **70**) and 53 to 100% (**71** to **72**)]. The laser stability of **71**/PMMA was only reduced to 67%, even after 400,000 pulses at 30 Hz. This indicates that covalent binding of the dye molecules to the polymer strands is an efficient way of increasing the stability of solid-state polymeric dye lasers.

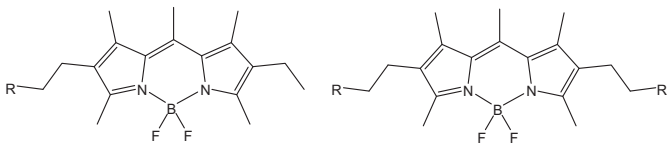

(**69**): R = CH_2OAc
(**70**): R = $CH_2OCOC(Me)=CH_2$
(**71**): R = CH_2OAc
(**72**): R = $CH_2OCOC(Me)=CH_2$

Fig. 42. BODIPYs bearing polymerisable substituents.

Polyphenylene derivatives of PM 567 were prepared containing the same functional groups as **69**–**72** in order to subject them to the same experiments of polymer doping and use as co-monomers (**73**–**78**; Fig. 43).[111,112] Each of the derivatives had a lower fluorescence quantum yield than the parent dye, PM 567, likely to be due to partial rotation of the phenyl ring. Compounds **73**, **75** and **77** showed remarkably high laser efficiencies of 42, 66 and 80%, respectively, in ethyl acetate, showing a significant increase in lasing efficiency with increasing number of phenyl rings. Each of the acetyl derivatives was bound in a PMMA polymer at two different concentrations (1.5 and 0.8 mM) and the laser properties were observed. Each of the acetyl derivatives was found to have a higher laser efficiency and stability than PM 567 in a PMMA polymer. No significant difference in laser efficiency was observed upon increasing concentration, but the 1.5 mM mixtures displayed increased laser stability with **75** being the most stable (76% after 100,000 pulses). The laser efficiency of compounds **73**, **75** and **77** in a PMMA polymer was found to be 18, 31 and 24%, respectively, at 1.5 mM concentration. While a moderate increase in laser efficiency is observed on increasing the number of phenyl rings from one to two, the addition of another phenyl ring causes a reduction in laser efficiency. When used as a co-monomer with MMA, a reduction in laser efficiency and stability was observed for compounds **76** and **78**, while compound **74**/MMA exhibited a similar efficiency, but increased stability. While the reduction in laser efficiency is only slight, the decreased stability is more marked (from 82 to 67% for **76** and 81 to 66% for **78**). Compound **73** dissolved in PMMA was found to have the lowest stability of the series, but when used as a co-monomer with MMA it was found to have the highest stability of the series (96% for 1.5 mM **73** in MMA). Each of these derivatives

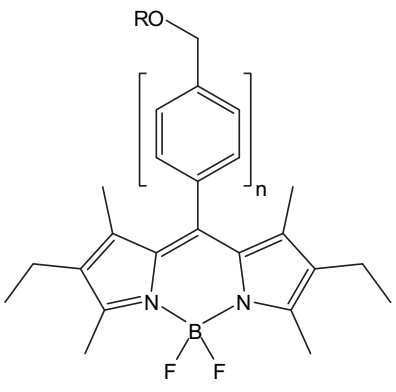

(**73**): n = 1; R = Ac
(**74**): n = 1; R = $COC(Me)=CH_2$
(**75**): n = 2; R = Ac
(**76**): n = 2; R = $COC(Me)=CH_2$
(**77**): n = 3; R = Ac
(**78**): n = 3; R = $COC(Me)=CH_2$

Fig. 43. 8-Phenyl analogues of PM 567.

showed increased laser efficiency over PM 567 when in liquid solution, in solid polymer solution, and when used as a component in a co-polymer.

Similar phenyl analogues of PM 597 have been prepared, which incorporate an acetyl (**79**) or an acrylate group (**80**) (Fig. 44).[113] The laser efficiency of **79** was calculated to be 52% in ethyl acetate, but this was reduced when dissolved in a solid polymer matrix. The highest laser efficiency for **79** was found for a PMMA solution (48%) with an impressive stability (98% at 10 Hz) with the stability being increased to 100% (10 Hz) in co-polymers 9:1 and 7:3 MMA/TMSPMA at the cost of further reduction in efficiency. Compound **82** exhibits a similar behaviour in PMMA solution (efficiency of 48%) with a slightly reduced stability (85%), which is increased to 100% in 1:1 MMA/HEMA along with a decrease in efficiency to 39%. Compounds **80** and **81** were dissolved in solid PMMA and were found to have moderate laser efficiency (46 and 38%, respectively) and stability (63 and 61%, respectively). PM 597 dissolved in solid PMMA displays higher efficiency than all the analogues in this series (52%) and higher stability than most (88% at 10 Hz). While the laser properties were reasonable (the laser stabilities being most impressive), the interesting aspect of this study was the colour tuning of the dyes, which were incorporated into the polymer matrices. Compound **80** emits in the green region, PM 597 emits in the yellow region and compound **79** emits in the orange/red region.

BODIPY emission has been shown to be promoted by electrochemical means, providing an alternative method of emission, despite lacking the sharp emission band of laser emission.[114] In this study, several commercial BODIPY dyes were investigated and were found to fluorescence via electrochemical excitation, albeit at a much weaker intensity. Commercial BODIPYs, PM 546, PM 567, PM 580 and PM 597, were studied and found to have fluorescence quantum yields of 0.95, 0.87. 0.85 and 0.41, respectively, when excited under conventional conditions. When excited via electrochemical means, a moderate red shift in the emission was observed (19–29 nm) at a very weak intensity (Φ_{ECL}=0.009, 0.007 and 0.003 for PM 567, PM 580 and PM 597, respectively. Electrochemical-promoted emission was not observed for PM 546).

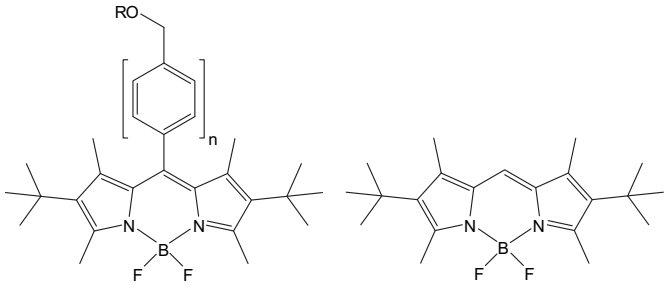

(**79**): n = 0; R = Ac
(**80**): n = 1; R = Ac
(**81**): R = COC(Me)=CH_2

82

Fig. 44. Analogues of PM 597.

4.2. Laser activity of BODIPYs in dye-doped liquid crystals

Commercially available BODIPY dyes have been used to dope nematic liquid crystals and have been shown to display laser behaviour similar to being dissolved in a solid polymer matrix. PM 597 has been used to dope BL 001 (commercially available nematic liquid crystal mixture—Merck), which has then been inserted into a wedge cell (two glass-ITO plates separated by Mylar spacers (100 μm) with the inner side of the plates being covered in rubbed polyimide alignment layers in order to induce homogeneous alignment of the nematic liquid crystal molecules).[115]

Photons absorbed by the dye 'guest' molecules are spontaneously re-emitted in random directions. Due to the random nature of this spontaneous emission, a significant amount of backscattering occurs from the sample. However, due to the thickness of the sample, these backscattered photons cause the spontaneous emission from other dye molecules before they leave the sample, resulting in a coherent chain reaction. When a population inversion is achieved, then the sample starts to lase. In ordinary lasers, the gain medium is suspended in an optical cavity and the pump beam is reflected back and forth through the cavity, but in this case the nematic host causes the system to act as a randomly distributed feedback laser, due to backscattering of the emitted photons. Due to the partially ordered nature of the nematic host, the dye molecules adopt some of the same ordering, allowing the emission to be controlled by varying the polarisation of the pump beam,[116] the laser emission being most intense when the pump beam is aligned parallel to the nematic director, and least intense when perpendicular to the director. The dye-doped BL 001 was also suspended in a glass capillary tube and was shown to lase with the same intensity as the sample in the wedge cell, but at red-shifted wavelengths and with additional intense lasing modes.[117] The laser intensity also showed a lower dependence on the polarisation of the pump beam than the aligned wedge cell sample, due to the less aligned nature of the nematic host in the capillary. The laser energy output was also measured as a function of temperature and was found to require increased pump pulse energy with increasing temperature, due to the decreased ordering of the nematic phase with increasing temperature. Both PM 597 and PM 650 in BL 001 have been freely suspended in a square-comb PVC net in order to produce thin films with laser activity.[118] Efficient laser emission was observed for both BODIPYs when freely suspended.

This random lasing in dye-doped liquid crystals has been exploited to produce lasing in a chiral nematic liquid crystal in a POLICRYPS-like grating.[119] A mixture of 'guest' PM 597 and 'host' BL 088 and NOA-61 was incorporated into a POLICRYPS system in which the dye-doped chiral nematic liquid crystal is placed into narrow parallel channels long enough for several helical periods to be passed through. This is not possible with the wedge-type cells, as their thickness is too short to allow any full helical periods to occur. By using a POLICRYPS system, each channel acts as a microcavity laser, due to the channels behaving as optical resonators. Stimulated emission occurs along the channels, emerging from the end of the channels when the incident pump beam is above a certain power. In this system, the wavelength was tunable by varying the temperature and the laser intensity by applying an electric field perpendicular to the helical axis.

5. Polymers incorporating BODIPY fluorophores

5.1. Polymerisation through the BODIPY core

BODIPYs have been incorporated into polymers through various linker groups and at various positions on the BODIPY to produce novel new fluorescent materials. The first co-polymers containing BODIPY fluorophores were prepared by Sonogashira coupling of a di-iodo-BODIPY to either a di-ethynyl-BODIPY or a phenylene co-monomer (**83**–**86**; Fig. 45).[120]

The polydispersity index (PDI) of compound **83** was the lowest of the series (1.27), while that of compound **84** was the highest (1.65). Compound **83** also possessed the lowest thermal decomposition temperature (200 °C) and compound **84** the highest (240 °C). The absorption and emission of this series of polymers were red shifted relative to the BODIPY monomer, presumably due to the extended conjugation through the BODIPY core. Due to the presence of two iodo substituents on the BODIPY monomer core, the fluorescence quantum yield for this unit is very low (0.02), but

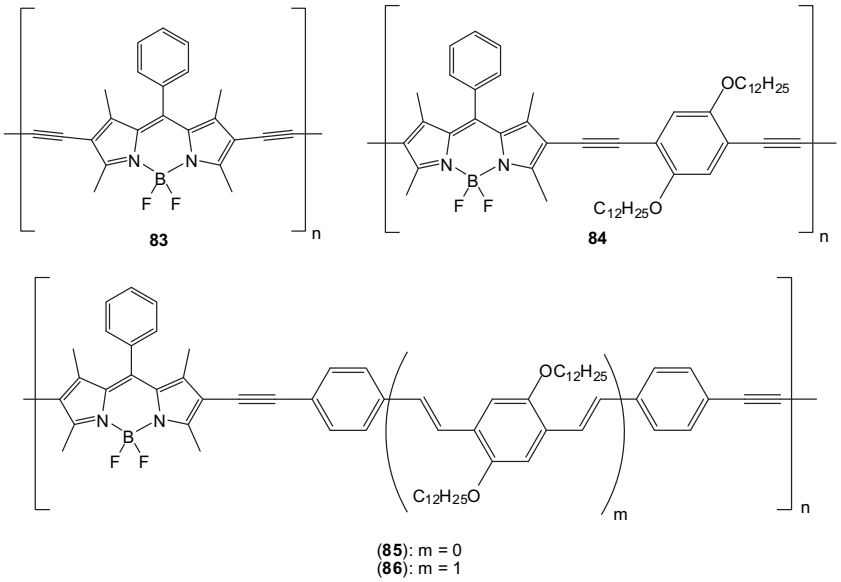

Fig. 45. BODIPY polymers with ethynyl or ethynyl-phenyl linker groups.

the resulting polymers all possess higher quantum yields. Of this series of polymers, compound **84** has the lowest quantum yield (0.08), while those of the other co-polymers are all very similar (0.24, 0.25 and 0.25 for **83**, **85** and **86**, respectively). The extension of the π-conjugate system also has the effect of reducing the oxidation potential.

The effect that the linker group, or lack thereof, has on the photophysical properties of a BODIPY-containing polymer has been investigated by employing various metal-catalysed cross couplings.[121] Yamamoto, Suzuki and Sonogashira couplings were all used to prepare a series of BODIPY-containing polymers from the same starting BODIPY monomer (**87**–**89**; Fig. 46). The PDIs of these polymers were 3.48, 3.15 and 3.02 for compounds **87**, **88** and **89**, respectively, and their decomposition temperatures all exceeded 310 °C. Compound **87** displayed a remarkably high extinction coefficient of 475,000 M^{-1} cm^{-1} and a relatively intense fluorescence (Φ_F=0.57). However, as the excitation and emission maxima are approximately the same as those for the monomer, it is assumed that there is little interaction between adjacent fluorophores along the polymer chain. This effect is consistent with a perpendicular arrangement of the fluorophores caused by the methyl groups on the BODIPY cores forcing each adjacent fluorophore out of co-planarity. Compound **88** displayed an unusually hypsochromically shifted absorption and emission spectrum (λ_{ex}=325 nm, λ_{em}=385 nm) and a much lower fluorescence quantum yield of 0.03. Compound **89** displayed a moderate fluorescence intensity (Φ_F=0.24), but a very low extinction coefficient (20,000 M^{-1} cm^{-1}). It also showed broad absorption and emission bands, due to aggregation of the polymer strands, even in dilute solutions.

The effects that different groups have on the photophysical properties of a BODIPY-containing polymer have been explored by altering the groups on the BODIPY phenyl ring as well as by altering the linker group between the fluorophores.[122] By separating the fluorophores with ethynyl groups (**90** and **91**; Fig. 47), interactions between adjacent fluorophores can occur, and this causes a significant red shift for the polymers relative to the monomers. The quantum

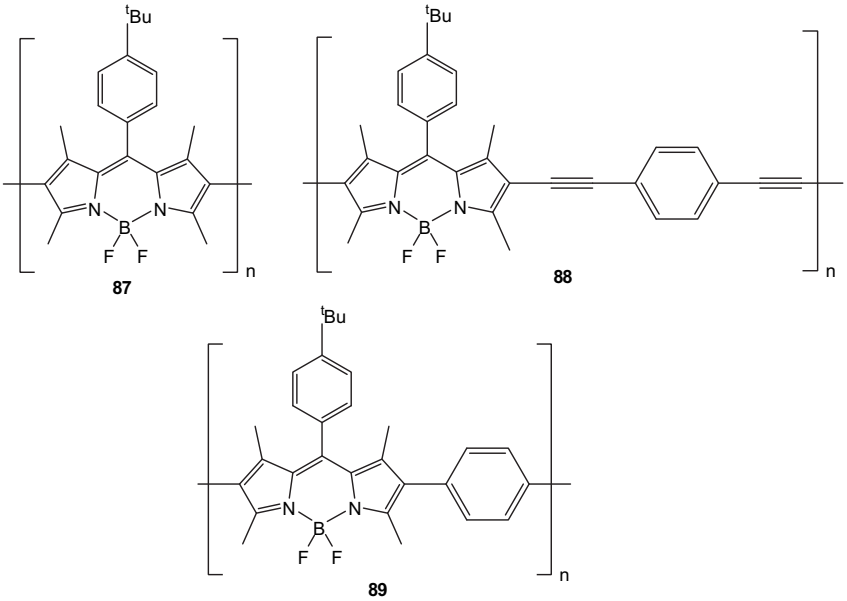

Fig. 46. BODIPY polymers with short or no linker groups.

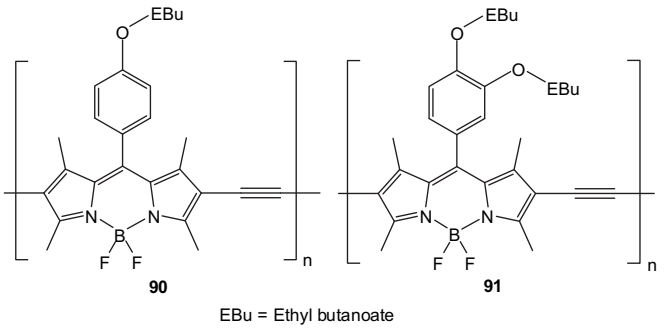

Fig. 47. BODIPY polymers with differing groups on the 8-phenyl ring.

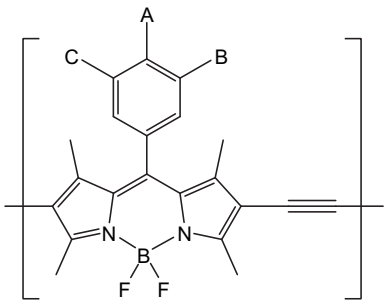

(**95**): A = $O(CH_2)_{11}Me$; B = C = H
(**96**): A = B = $O(CH_2)_{11}Me$; C = H
(**97**): A = B = C = $O(CH_2)_{11}Me$

Fig. 49. BODIPY polymers with increasing numbers of long alkyl chains.

yields are reduced upon polymerisation (0.21 and 0.23 for **90** and **91**, respectively); but compound **91** has a slightly higher quantum yield as well as being slightly more red shifted than compound **90**.

Interestingly, the absorption and emission spectra of compounds **92**–**94** (Fig. 48) were not as red shifted as those of compounds **90** and **91**, despite having an extended conjugate system. The differences in their emission wavelengths are consistent with the band-gap energy differences for the aromatic linker units. Compounds **92** and **93** have similar quantum yields (0.25 and 0.24, respectively), but compound **94** has a much lower quantum yield (0.06) and fluorescence lifetime (0.23 ns). This is presumably caused by the heavy-atom effect of the sulfur atom of the thiophene ring.

to decompose only above 300 °C. Polymer **94** and a similar analogue lacking the thiophene unit have been incorporated into a dye-sensitised solar cell device with PCBM and remarkable power conversion efficiencies (PCEs) have been observed.[124] Polymer **94**/PCBM 1:3 was found to have the highest PCE of the series investigated at 2.0% with a broad absorption profile, due to the extended delocalised π-system along with the UV absorption of the PCBM moiety. This broad absorption spectrum results in a broad photocurrent generation profile.

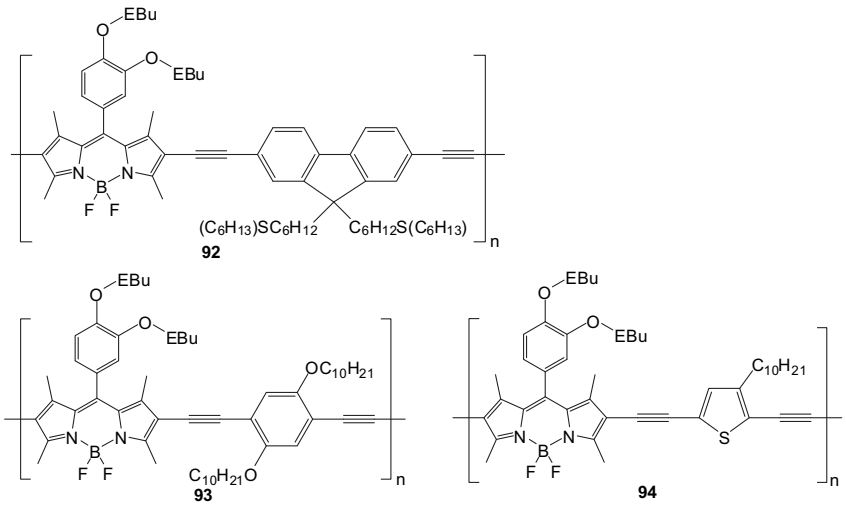

Fig. 48. BODIPY polymers with different types of linker group.

The number of alkyloxy substituents on the BODIPY phenyl ring can have a significant effect on the photophysical properties of a BODIPY-containing polymer, particularly when cast as a thin film.[123] As would be expected, the excitation and emission spectra of polymers **95**–**97** (Fig. 49) are significantly red shifted relative to the monomers, due to extended π-conjugation, and the fluorescence quantum yields are all similar (0.13–0.15). With increasing number of alkyloxy substituents, the excitation and emission of each polymer are further red shifted and the Stokes' shift is shortened. However, when cast as a thin film, the initial increase in the number of alkyloxy substituents causes a marked red shift in the excitation, but only slightly for the emission. While a thin film of compound **95** absorbs at 680 nm and emits at 723 nm, a thin film of compound **96** absorbs at 728 nm and emits at 741 nm. However, compounds **96** and **97** have very similar excitation and emission profiles. Each of these polymers is relatively thermostable, starting

The effect that different substituents on the BODIPY phenyl ring have on the photophysical properties of BODIPY-containing polymers has been further investigated through the preparation of polyfluorene–BODIPY polymers (**98**–**100**; Fig. 50).[125] As seen in previous examples, the extension of the π-system delocalisation results in a bathochromic shift in the polymer absorption relative to the monomer. Electron-donating methoxy groups have a slight effect on the absorption, but there is an even lesser effect on the emission (**98** and **99**), while the methyl groups cause an increase in fluorescence quantum yield (**100**). Interestingly, polymers **98** and **100** were found to be sensitive to both fluoride and cyanide anions. Both polymers displayed a decreased BODIPY absorption and emission intensity with increasing concentration of fluoride and cyanide anions, and they also displayed a concurrent hypsochromic shift in the absorption wavelength. This may be due to decomposition of the BODIPY core caused by fluoride anions.[14,126]

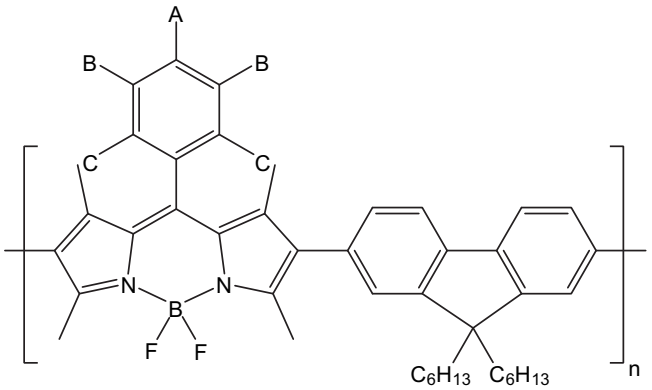

(**98**): A = B = OMe; C = H
(**99**): A = OMe; B = C = H
(**100**): A = B = H; C = Me

Fig. 50. Fluorene-linked BODIPY polymers.

Cyanide anions were shown to decrease the absorption peak of the BODIPY, but a new absorption band was not observed, indicating that cyanide anions are not as damaging to the BODIPY core as fluoride anions. The anion size seems to play an important role in the function of these polymers as sensors, as no response was observed for chloride, bromide or iodide anions.

BODIPYs, which already display absorption and emission in the red region have also been incorporated into polymers and have been shown to undergo a further red shift when polymerised (**101**–**103**; Fig. 51).[127] While each of the polymers **101**–**103** absorbs and emits in the red region, the presence and position of the methoxy group have a moderate effect on the absorption, emission and quantum yield. Polymer **102** is slightly hypsochromically shifted (15 nm) but displays a more intense fluorescence relative to **101** (0.49, compared to 0.33), while **103** is bathochromically shifted (17 nm) with only a slightly increased quantum yield (0.38, compared to 0.33). Each of the polymers is red shifted, compared to their respective monomers, due to extension of the π-system delocalisation. All the polymers start to decompose above 275 °C.

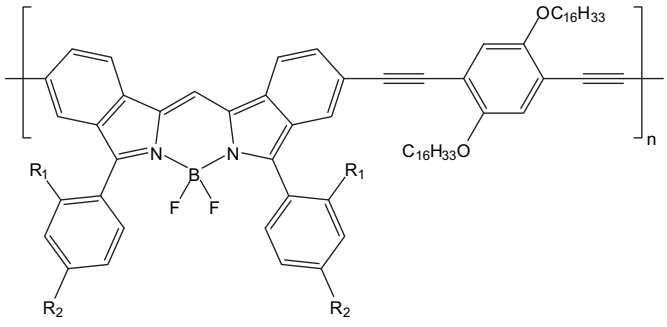

(**101**): $R_1 = R_2 = H$
(**102**): $R_1 = OMe$; $R_2 = H$
(**103**): $R_1 = H$; $R_2 = OMe$

Fig. 51. BODIPY polymer with red-shifted absorption and emission.

5.2. Polymerisation through F-substitution

Polymerisation of BODIPYs through palladium-catalysed cross coupling on the BODIPY core itself causes a red shift in the fluorescence, but this effect can be tempered by polymer formation through fluorine substitution. These systems were initially investigated using relatively linear aryl groups (**104**–**106**; Fig. 52).[128] The fluorescence quantum yields of these polymers were all relatively intense (0.80, 0.71 and 0.85 for **104**, **105** and **106**, respectively), while the absorption and emission for each polymer were very similar to those of the monomer. The emission was found to red shift and the peak to broaden when the polymers were cast as thin films. The most interesting property of these polymers, however, was found to be their self-assembly behaviour. Polymer **104** was found to form nm-sized particles and μm-sized fibres by aggregation of the polymer strands. Polymer **105** was found to display a preference for particles over fibres, while polymer **106** displayed almost no fibre-like structures. This suggests that the fibre-like structures are a result of steric interactions of the aryl linker groups.

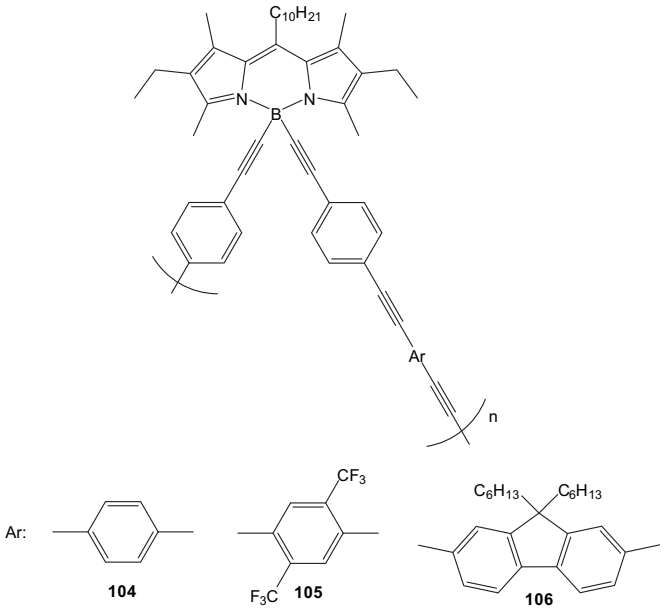

Fig. 52. BODIPY polymers prepared via F-substitution.

This type of BODIPY polymerisation has been used to prepare a chiral BODIPY polymer with *S*- and *R*-6,6′-diethynyl-2,2′-dioctyloxy-1,1′-binaphthyl as the chiral linker (**107**; Fig. 53).[129] The absorption and emission of each diastereomer were found to be identical, as well as to those of the monomer. Both the *R*- and *S*-polymers displayed a tendency to form fibre-like structures through aggregation of particles, but fibre formation was found to be disrupted by the addition of the other diastereomer, with 3:7*S*:*R* showing complete disruption of fibre formation, and consequently only particles were observed. This was attributed to the disruption of particle aggregation caused by the presence of the opposite diastereomer.

5.3. Polymerisation through the BODIPY 8-position

While polymerisation of BODIPYs through the BODIPY core itself can induce a red shift in the absorption and emission of the resulting polymer and polymerisation via F-substitution can lead to interesting molecular architectures, attaching a monomer to a BODIPY through a simple linker can provide a polymer containing ancillary BODIPY fluorophores. HEMA monomer analogues have been attached to BODIPY fluorophores (**108**) (Fig. 54) and a hybrid polymer has been prepared by reaction with MeTMOS.[130]

Polymers of this type were prepared through both microwave and conventional heating, as well as with differing molar ratios of BODIPY-HEMA/HEMA, and interesting results were observed. By increasing the ratio of the BODIPY–HEMA conjugate, it was

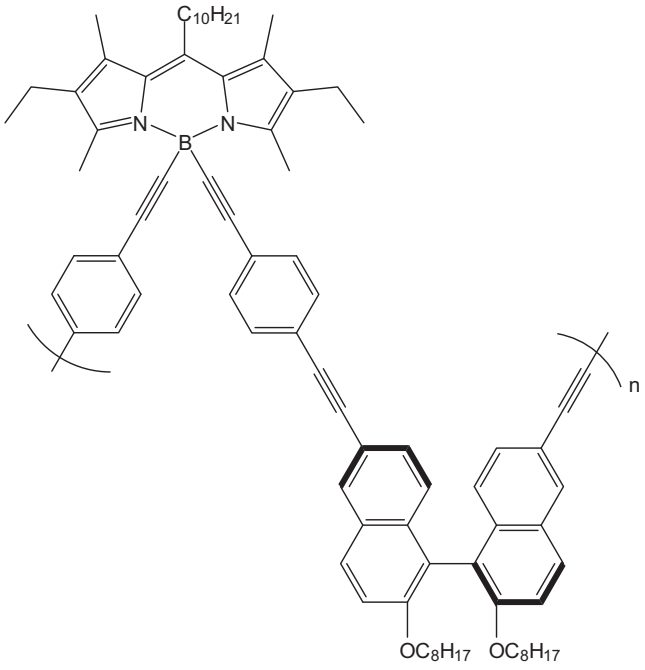

107

Fig. 53. Chiral BODIPY polymer.

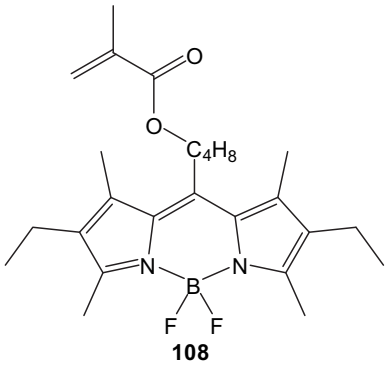

108

Fig. 54. BODIPY/HEMA analogue.

observed that the fluorescence quantum yield of the resulting polymer was lower than that of a less concentrated mixture. This fluorescence quenching was attributed to aggregation of the fluorophores and the formation of H-dimers. It was also observed that, on the whole, the microwave-assisted polymerisation reactions produced polymers with slightly higher quantum yields than via conventional heating. This led to a different mechanism of polymer assembly being proposed for each heating method. It was observed that microwave heating discouraged aggregation of the polymer strands, and thus disrupted aggregation of the fluorophores causing a higher quantum yield. Similar to the F-substitution polymers, these hybrid polymers displayed very similar fluorescence to that of their respective monomer.

Similar co-polymers have been prepared by the reaction of a BODIPY/HEMA analogue with 2-(dimethylamino)ethyl methacrylate (DMAEMA) intercalated between terminal units of cumyl dithiobenzoate (CDB) (**109**; Fig. 55).[131] The most useful aspect of this polymer is its solubility in water. The fluorescence intensity of these polymers was observed to increase with increasing temperature, making them useful as water-soluble thermometers. This fluorescence increase is thought to be due to decreasing fluorophore aggregation with increasing temperature. Polymers **109** as

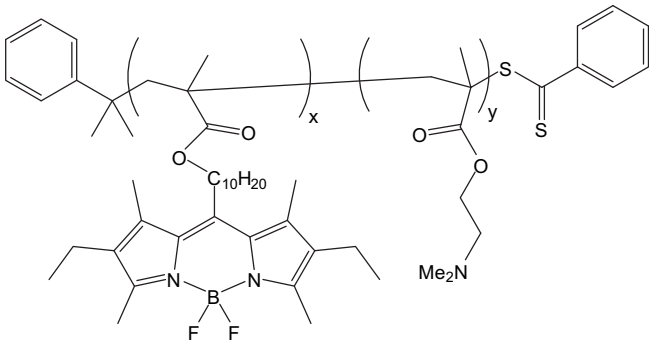

109

Fig. 55. BODIPY/HEMA polymer.

well as an analogue containing ethynyl-phenyl groups on the boron atom were found to adopt particular structures.[132]

The same effect was observed for a BODIPY-containing polymer formed by a quaternary pyridinium-BODIPY (**110**; Fig. 56).[133] Below 23 °C, the fluorescence of the polymer was very weak, but a fivefold increase in fluorescence intensity was observed upon increasing the temperature to 35 °C, at which no further increase was observed (Φ_F=0.262). This fluorescence increase is promoted by heat-induced polymer aggregation, which causes the formation of viscous microdomains, suppressing the rotation of the BODIPY pyridinium ring. This polymer was found to be stable enough to be used as a fluorescent thermometer at least ten times.

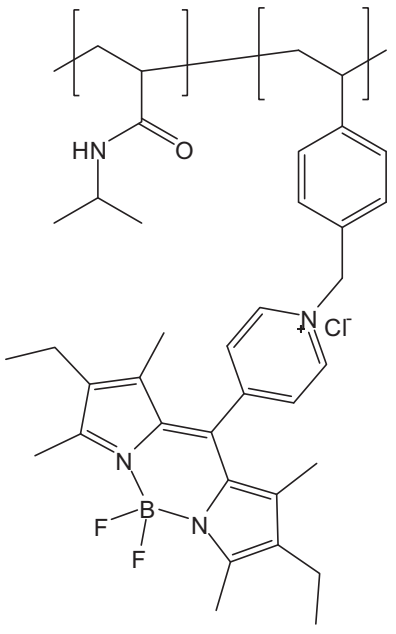

110

Fig. 56. BODIPY polymer bearing quaternary pyridinium moiety.

5.4. Polymerisation through metal complexation and conducting polymers

A novel BODIPY-containing polymer was prepared by using zinc-terpyridine as a linker group (**111**; Fig. 57).[134] A gradual fluorescence increase was observed upon titration of the uncomplexed form with zinc(II) triflate, indicating the formation of the polymer. Two absorption peaks in the UV region also became more intense with increasing coordination polymer formation. Zinc coordination could be observed by the ^{1}H NMR peaks becoming sharper with

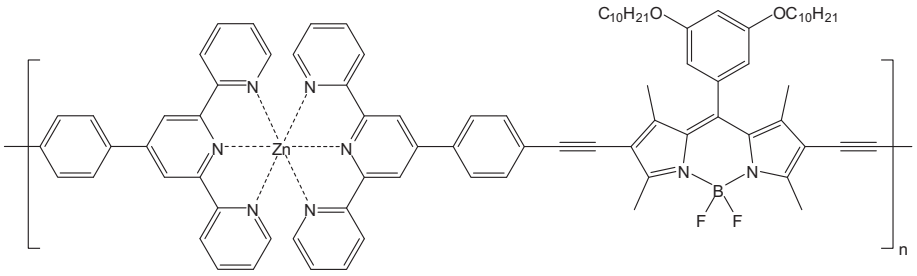

111

Fig. 57. BODIPY–terpyridine–zinc coordination polymer.

increasing amounts of zinc. This particular type of polymer could find use in electrochromic devices.

As seen previously, BODIPYs can be used as components in novel photovoltaic devices. This work has been extended to the preparation of conducting BODIPY polymers. The initial investigations into conducting BODIPY polymers were carried out using a polythiophene/pyrrole–BODIPY system (**112**; Fig. 58).[135] It was found that this polymer adopted 'cauliflower-like' structures in solution, indicating that polymer growth takes place after initial nucleation. Significant changes in transmittance were observed when the polymer was switched between −0.2 and 1.2 V electric fields. A clearly visible colour change was also seen upon switching between −1.3 and 1.1 V (red, pink, blue and green at −1.3, 0.0, 0.8 and 1.1 V, respectively).

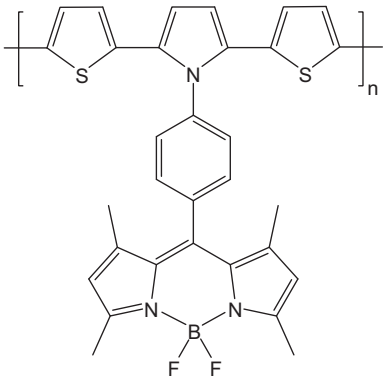

112

Fig. 58. Conducting BODIPY polymer.

A donor–acceptor polymer has been prepared incorporating a BODIPY acceptor and 3,4-ethylenedioxythiophene (EDOT) donor (**113**; Fig. 59).[136] As seen for the previous conducting polymer (**112**), a colour change was observed upon oxidation from violet (neutral) to indigo (oxidised). A clear increase in the absorption in the IR region (two-photon absorption) was seen with increasing applied voltage. A red shift in the absorption was also observed upon conjugation of the EDOT units, due to extension of the delocalised π-system.

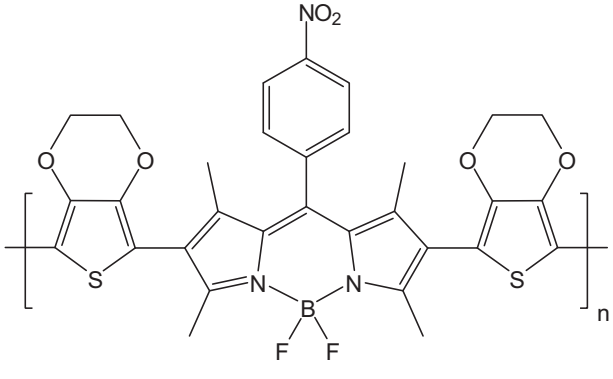

113

Fig. 59. Conducting BODIPY polymer with extended π-conjugation.

An analogue of **113** containing thiophene units between the EDOT groups has been prepared and a slight red shift in the absorption was observed with increasing applied potential.[137] A clear colour change from pink to blue was also observed upon oxidation. A more straightforward relationship between applied potential and absorption was observed for this analogue. A gradual decrease in BODIPY absorption with a concurrent increase in absorption in the IR region (two-photon absorption) was observed with increasingly positive applied potential. Similar structures to those of **113** were observed under scanning electron microscopy.

6. Mesogenic BODIPYs and their self-assembling properties

Because of their remarkable fluorescent properties, BODIPYs have been attracting increasing interest as self-assembling materials, particularly liquid crystals, due to their increasingly common usage in display devices. BODIPYs were initially found to adopt columnar phases when appended with multiple alkyl chains.[138,139] In this study, two discotic liquid crystals were prepared, one of which had the mesogenic unit further away from the BODIPY core (**114** and **115**; Fig. 60). Four analogues of **114** were prepared, where n=1, 8, 12 and 16, while only the n=8, 12 and 16 analogues of **115** were synthesised. Each of the **114** analogues (other than n=1) exhibited a hexagonal columnar phase (Col_h) with gradually decreasing melting points and phase transitions, but widening columnar range with increasing chain length. The same effects were observed for the n=12 and 16 analogues of **115** (the n=8 analogue did not display a mesophase). Several of the compounds also displayed crystal–crystal transitions, and decomposition occurred when the n=8 analogue of **114** was heated above 250 °C.

A fan-like texture was observed in the hexagonal columnar phase when viewed under crossed polarisers and this texture could still be seen when irradiated at 300–350 nm and not viewed under crossed polarisers. Both these images were superimposed onto one another and it appeared that emission of the BODIPY in the liquid crystalline state was related to the different molecular orientations when in the mesophase. A red shift was also observed in the transition from the mesophase to the crystalline phase, due to the formation of aggregates. These compounds were shown to undergo efficient gelation in nonane to form highly luminescent gels. An n=17 analogue of compound **114** was found to exhibit electrogenerated chemiluminescence when excited with an applied electric field or with a co-reactant (benzoyl peroxide).[140]

A series of BODIPYs with similar structures to compound **114** have also been prepared and, while lacking mesophase formation, have been shown to readily form thin films (**116**; Fig. 61).[141] As seen for several of the BODIPY-containing polymers, it is the alkyl chains

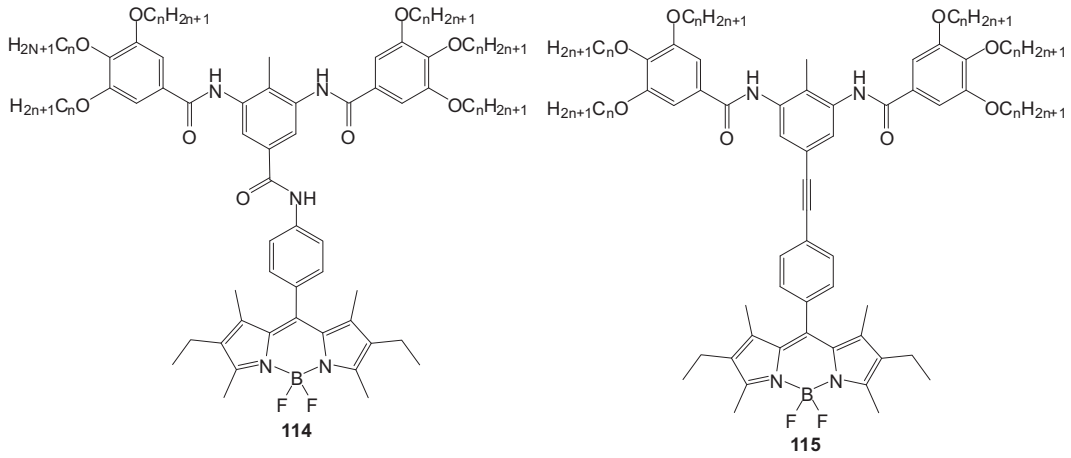

Fig. 60. Discotic BODIPYs.

that promote this thin film formation. Electrogenerated chemiluminescence was observed for these compounds, making them potentially useful in organic LEDs (OLEDs).

An analogous monomesogenic BODIPY was also prepared, which, despite displaying birefringence, did not exhibit any mesophase formation (**117**; Fig. 62).[142] As with the analogues of compound **116**, analogues of **117** were found to form thin films and undergo electrogenerated chemiluminescence. It was observed that, by using a higher voltage to generate chemiluminescence, the resulting luminescence intensity increased.

The first example of a BODIPY exhibiting the nematic phase was observed for a relatively small molecule, consisting of a BODIPY conjugated to a cyanobiphenyl by an alkyl chain (**118**; Fig. 63).[143] This compound displayed a remarkably stable (90 °C) enantiotropic nematic phase between 47 and 137 °C. Interestingly, both the BODIPY and the uncomplexed mesogenic dipyrrin displayed nematic behaviour, with the BODIPY having slightly higher crystal-to-nematic and nematic-to-isotropic transition temperatures (41 and 132 °C for the uncomplexed dipyrrin and 47 and 137 °C for the BODIPY). A mesogenic bis(dipyrrinato)-nickel complex also displayed nematic behaviour, but as a monotropic phase between 134 and 119 °C.

Since this initial discovery, nematic behaviour has been conferred on BODIPYs by attaching them to liquid crystalline dendrimers.[144] A series of first-, second- and third-generation liquid crystalline dendrimers (Fig. 64) were prepared and attached to a highly fluorescent BODIPY core, with both nematic and smectic A behaviour being observed for the resulting mesogenic BODIPYs. The first-generation BODIPY-dendrimer exhibited a nematic phase, as well as a mesophase that could not be identified. This transition from the crystal to the unknown mesophase occurred at 86 °C, followed by transition into a short-lived nematic phase at 119 °C, before melting into the isotropic liquid at 123 °C. Nematic behaviour was not observed for either the second- or third-generation BODIPY-dendrimers, with only smectic A phases being exhibited for these compounds. The transition from the second- to the third-generation dendrimer caused a reduction in the crystal-to-smectic A transition temperature (100–83 °C) and an increase in the

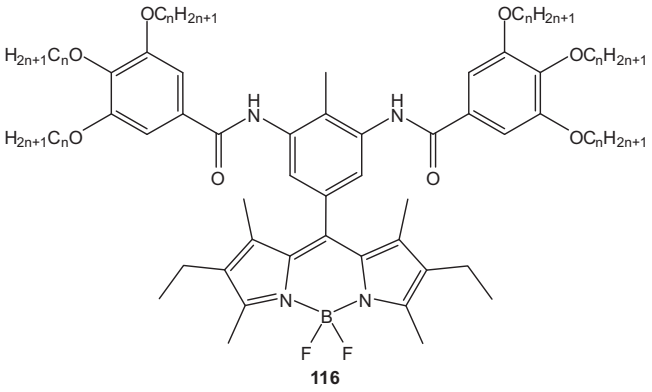

Fig. 61. Discotic BODIPY, which forms thin films.

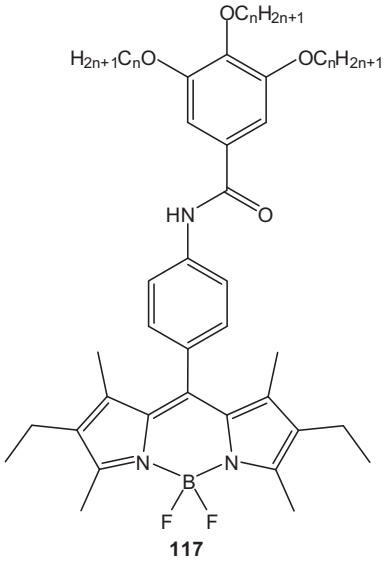

Fig. 62. Chemiluminescent BODIPYs.

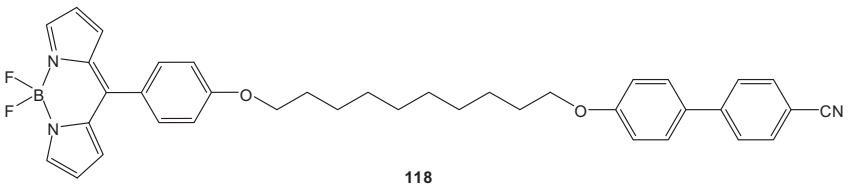

Fig. 63. Mesogenic BODIPY exhibiting nematic phase behaviour.

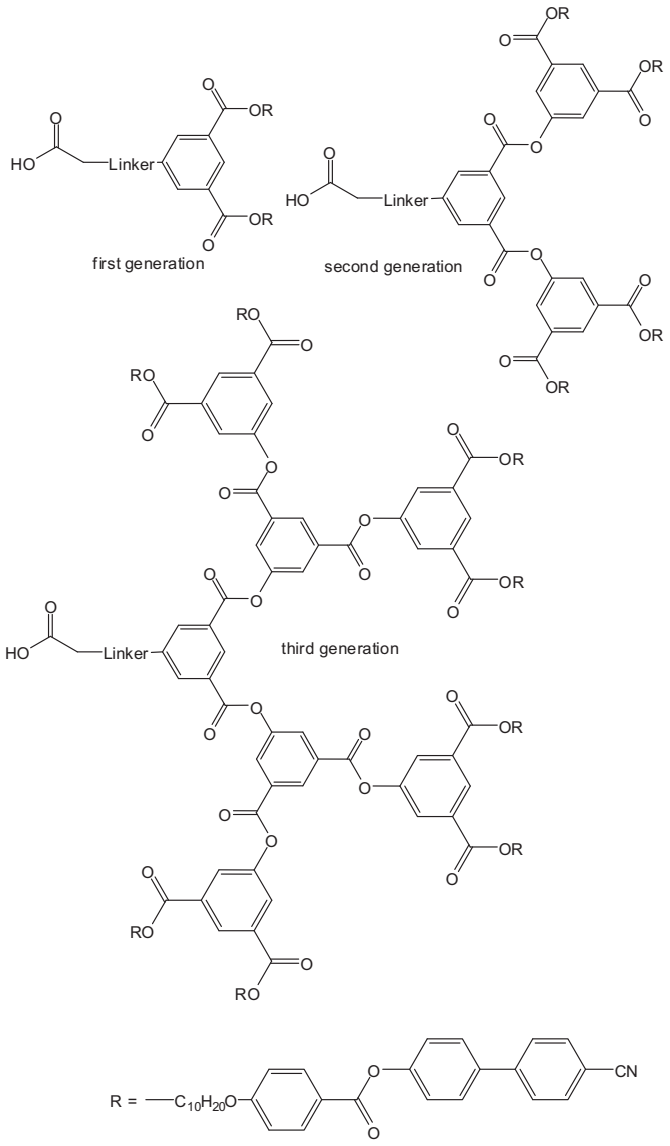

Fig. 64. Liquid crystalline dendrimers for attachment to BODIPYs.

mesophase transition enthalpies and a concurrent increase in the enthalpy contribution per mesogenic unit. For this series of compounds, it was proposed that the BODIPY fluorophores aggregated into sub-layers, with the dendritic units forming layers above and below the layer of BODIPYs, with interdigitation occurring between the dendritic units of adjacent layers. Like BODIPY polymer **110**, temperature-dependent fluorescence studies were carried out on the molecules in the crystal, nematic, smectic A and isotropic liquid phases, but no significant change in the fluorescence intensity was observed when going from one mesophase to the next.

Ionic liquid crystals have been prepared based on BODIPYs bearing sulfonate units ionically bound to gallate-based mesogens (**119**; Fig. 65).[145] Three different alkyl chain lengths were employed to investigate the self-assembly behaviour of these compounds (n=12, 14 and 16). Each analogue was found to decompose above 180 °C and to display a slightly shorter hexagonal columnar range with increasing chain length. The columnar range was still found to be very wide, being over 160 °C for each compound. It was suggested that each disc in the hexagonal columnar phase consisted of centrally aggregated BODIPY units surrounded by the mesogenic units. This was the first example of a BODIPY-based ionic liquid crystal as well as the first example of a BODIPY-based liquid crystal in which the mesogenic units were not attached to the central position of the BODIPY fluorophore.

This work was extended to prepare BODIPY-based ionic liquid crystals with the same gallate-based mesogen, but coordinated to the sulfonate groups by imidazole groups (**120**; Fig. 66).[146] Three analogues of compound **120** were prepared (n=8, 12 and 16) and each exhibited a hexagonal columnar phase. Similar transition temperatures were determined for each of the analogues with a fan-like texture being observed when viewed under crossed polarisers. As for compound **119**, it was proposed that the BODIPY units aggregate together and the mesogenic units form a disc-like shape around them. An n=12 analogue was prepared, which terminated in a methacrylate group and was polymerised via a photoinduced mechanism. The resulting polymer was found to form thin films and to be highly chemically stable, even in the presence of the radicals generated during the polymerisation process.

A polymer-dispersed nematic liquid crystal host has been doped with a simple BODIPY dye to study the alignment of the dye molecules relative to the host material.[147] Reorientation of the dye molecules was proposed to occur by interactions with both the host

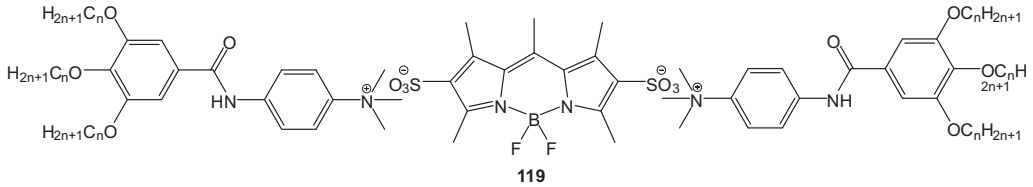

119

Fig. 65. Ionic BODIPY liquid crystal formed by interactions between quaternary ammonium and sulfonate groups.

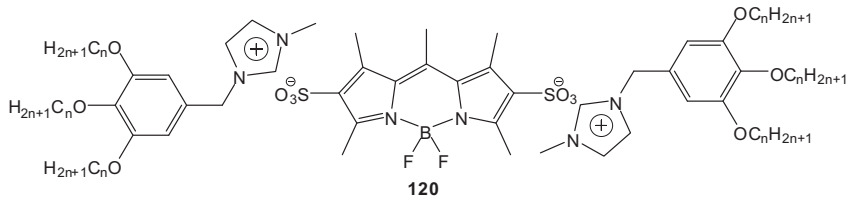

120

Fig. 66. Ionic BODIPY liquid crystal formed by interactions between imidazole and sulfonate groups.

smectic A-to-isotropic transition temperature (155–211 °C), resulting in an increase in the smectic A stability. Each increase in the number of mesogens caused an increase in the crystal-to-material and directly with the electric field. The two reorientation mechanisms cause a rotation of the dye alignment axis, thus causing a change in the fluorescence intensity, due to rotation of

the dye transition dipole moment. This rotation of the dye transition dipole moment caused a reduction in the fluorescence intensity when the electric field was switched on. The drop in fluorescence intensity was not a clear ON/OFF switching, but rather a reduction by approximately 60 counts when the electric field was on. Due to the dye molecules being a very dissimilar shape to the nematic host material, they only align with the host weakly and, so, while this initial study lays the groundwork for further research, BODIPYs that align more strongly with the host material may display very different properties.

7. Conclusions

The remarkable fluorescence properties of BODIPYs give them great potential as photoactive materials. Increasing interest in the chemistry of BODIPYs is helping to fuel the number of applications for which they can be used, including non-material-based applications, such as chemosensors[4,6,13,148,149] and as imaging agents.[17,150–154] BODIPYs have even started to find applications as photodynamic therapy agents,[19–21] usually considered to be the primary application of porphyrins and phthalocyanines.

The high efficiency of energy transfer from and to BODIPY dyes has allowed them to find applications in energy transfer arrays and, hence, solar cells. They exhibited surprisingly high power conversion efficiencies in both bulk-heterojunction solar cells as well as dye-sensitised solar cells. While BODIPYs for BHJs display efficient photocurrent generation, they tend to require groups that promote film formation (e.g., PEG). BODIPYs for titanium dioxide sensitisation, however, just require a group that enables binding to the inorganic material (e.g., carboxyl). While this would seem to make dye-sensitising agents a more attractive prospect for photocurrent generation, the increasing use of organic materials like BHJs is promoting further research into BODIPYs as BHJ components.

Due to their intense fluorescence and high photostability, BODIPYs can also be used as laser dyes with remarkably high efficiencies in some cases. This laser activity has prompted several groups to dissolve the dyes in a solid polymer matrix, in which the dyes lase with a lower efficiency than in liquid solution, but with a higher stability. The BODIPYs remain laser active, even when dissolved in a semi-ordered material like a nematic liquid crystal. The dye molecules have been shown to align weakly with the host material and lasing has been observed when the dye-doped material is incorporated into an optical cell or capillary tube, and when freely suspended. Due to the prevalence of the polymer and liquid crystal host materials, and the commercial availability of a range of BODIPY dyes, laser activity studies of this type are the most easily accessed area of materials research for BODIPYs.

While commercial BODIPY dyes can be readily dissolved in a polymer matrix, the incorporation of BODIPY fluorophores into the polymer backbone itself requires greater synthetic consideration. It has been shown by several groups that BODIPYs can be incorporated into a polymer chain by attachment through the BODIPY core, by fluorine substitution, or through the BODIPY 8-position. This leads to a wide variety of polymers with a range of self-assembling and photophysical properties. These polymers can also be cast as thin films, which possess different photophysical properties to those of the BODIPY polymer in solution, allowing colour tuning to take place, even after the synthesis of the molecule is complete. Polymerisation has even been shown to occur through metal complexation when the appropriate ancillary ligands are attached. Due to the delocalised π-system and efficient energy-transfer processes that can occur in BODIPYs, conducting polymers can be prepared, which show high sensitivity to an applied electric field (electrochromism), making them potentially useful as molecular switches.

More recently, attempts have been made to incorporate the BODIPY fluorophore into a liquid crystalline molecule. Initially, discotic-type molecules were prepared, some of which exhibited hexagonal columnar phases, while others could be cast as thin films, but did not display any mesophase behaviour. The first example of a BODIPY-containing nematic liquid crystal was reported by Boyle et al.[143] and consisted of a BODIPY fluorophore conjugated to a cyanobiphenyl mesogen. Despite being a relatively simple mesogen, the resulting mesogenic BODIPY exhibited a wide-range nematic phase at moderate temperatures. Liquid crystal dendrimers terminating in cyanobiphenyl units have also been employed to induce liquid crystallinity onto a BODIPY quite effectively, but require additional synthetic steps for dendrimer synthesis. Ionic liquid crystals have also been prepared, which exhibited hexagonal columnar phases with each disc being formed from aggregated BODIPYs surrounded by mesogenic units. These results illustrate that BODIPYs have promise as fluorescent liquid crystals; although this particular area of research is still in its infancy and further work is required before BODIPY-based liquid crystals find their way into optoelectronic devices.

There are a growing number of reactions that can be carried out on BODIPY dyes, with each one affecting the photophysical properties of the dye in reasonably specific ways, and these reactions are being exploited in the preparation of new BODIPY-based materials. The recent synthesis of the core BODIPY dye (fully unsubstituted) finally allows each new BODIPY and BODIPY-based material to be compared to a relevant standard. These factors, plus the increasing interest in organic materials, are fuelling the preparation of new photoactive materials based on BODIPY dyes, primarily for the production of highly sensitive optoelectronic devices and more efficient solar cells.

References and notes

1. Loudet, A.; Burgess, K. *Chem. Rev.* **2007**, *107*, 4891–4932.
2. Wood, T. E.; Thompson, A. *Chem. Rev.* **2007**, *107*, 1831–1861.
3. Ulrich, G.; Ziessel, R.; Harriman, A. *Angew. Chem., Int. Ed.* **2008**, *47*, 1184–1201.
4. Jiang, J. L.; Lu, H.; Shen, Z. *Chinese J. Inorg. Chem.* **2010**, *26*, 1105–1108.
5. Atilgan, S.; Ozdemir, T.; Akkaya, E. U. *Org. Lett.* **2008**, *10*, 4065–4067.
6. Lu, H.; Xiong, L.; Liu, H.; Yu, M.; Shen, Z.; Li, F.; You, X. *Org. Biomol. Chem.* **2009**, *7*, 2554–2558.
7. Kim, H. J.; Kim, J. S. *Tetrahedron Lett.* **2006**, *47*, 7051–7055.
8. Koutaka, H.; Kosuge, J. I.; Fukasaku, N.; Hirano, T.; Kikuchi, K.; Urano, Y.; Kojima, H.; Nagano, T. *Chem. Pharm. Bull.* **2004**, *52*, 700–703.
9. Wang, D.; Shiraishi, Y.; Hirai, T. *Tetrahedron Lett.* **2010**, *51*, 2545–2549.
10. Lu, H.; Zhang, S.; Liu, H.; Wang, Y.; Shen, Z.; Liu, C.; You, X. *J. Phys. Chem. A* **2009**, *113*, 14081–14086.
11. Du, J.; Fan, J.; Peng, X.; Li, H.; Wang, J.; Sun, S. *J. Fluoresc.* **2008**, *18*, 919–924.
12. Tian, M.; Peng, X.; Fan, J.; Wu, Y. *Chin. J. Anal. Chem.* **2006**, *34*, S283–S288.
13. Rao, M. R.; Mobin, S. M.; Ravikanth, M. *Tetrahedron* **2010**, *66*, 1728–1734.
14. Coskun, A.; Akkaya, E. U. *Tetrahedron Lett.* **2004**, *45*, 4947–4949.
15. Fan, J.; Guo, K.; Peng, X.; Du, J.; Wang, J.; Sun, S.; Li, H. *Sens. Actuators, B* **2009**, *142*, 191–196.
16. Shiraishi, Y.; Maehara, H.; Sugii, T.; Wang, D.; Hirai, T. *Tetrahedron Lett.* **2009**, *50*, 4293–4296.
17. Saito, R.; Ohno, A.; Ito, E. *Tetrahedron* **2010**, *66*, 583–590.
18. Alamiry, M. A. H.; Benniston, A. C.; Copley, G.; Elliott, K. J.; Harriman, A.; Stewart, B.; Zhi, Y. G. *Chem. Mater.* **2008**, *20*, 4024–4032.
19. Yogo, T.; Urano, Y.; Ishitsuka, Y.; Maniwa, F.; Nagano, T. *J. Am. Chem. Soc.* **2005**, *127*, 12162–12163.
20. Lim, S. H.; Thivierge, C.; Nowak-Sliwinska, P.; Han, J.; Van Den Bergh, H.; Wagniares, G.; Burgess, K.; Lee, H. B. *J. Med. Chem.* **2010**, *53*, 2865–2874.
21. Erbas, S.; Gorgulu, A.; Kocakusakogullari, M.; Akkaya, E. U. *Chem. Commun.* **2009**, 4956–4958.
22. Wang, J. G.; Li, Z. B.; Hou, Y. J.; Zhang, B. W.; Wang, X. S. *Imaging Sci. Photochem.* **2010**, *28*, 279–286.
23. Ozlem, S.; Akkaya, E. U. *J. Am. Chem. Soc.* **2009**, *131*, 48–49.
24. Shiragami, T.; Tanaka, K.; Andou, Y.; Tsunami, S. I.; Matsumoto, J.; Luo, H.; Araki, Y.; Ito, O.; Inoue, H.; Yasuda, M. *J. Phtochem. Photobiol. A* **2005**, *170*, 287–297.
25. Liu, J. Y.; Ermilov, E. A.; Roder, B.; Ng, D. K. P. *Chem. Commun.* **2009**, 1517–1519.
26. Liu, J. Y.; Yeung, H. S.; Xu, W.; Li, X.; Ng, D. K. P. *Org. Lett.* **2008**, *10*, 5421–5424.
27. Paul, D.; Wytko, J. A.; Koepf, M.; Weiss, J. *Inorg. Chem.* **2002**, *41*, 3699–3704.
28. Koepf, M.; Trabolsi, A.; Elhabiri, M.; Wytko, J. A.; Paul, D.; Albrecht-Gary, A. M.; Weiss, J. *Org. Lett.* **2005**, *7*, 1279–1282.
29. Maligaspe, E.; Tkachenko, N. V.; Subbaiyan, N. K.; Chitta, R.; Zandler, M. E.; Lemmetyinen, H.; D'Souza, F. *J. Phys. Chem. A* **2009**, *113*, 8478–8489.
30. Maligaspe, E.; Kumpulainen, T.; Subbaiyan, N. K.; Zandler, M. E.; Lemmetyinen, H.; Tkachenko, N. V.; D'Souza, F. *Phys. Chem. Chem. Phys.* **2010**, *12*, 7434–7444.

31. Ziessel, R.; Allen, B. D.; Rewinska, D. B.; Harriman, A. *Chem.—Eur. J.* **2009**, *15*, 7382–7393.
32. Yilmaz, M. D.; Bozdemir, O. A.; Akkaya, E. U. *Org. Lett.* **2006**, *8*, 2871–2873.
33. Bozdemir, O. A.; Yilmaz, M. D.; Buyukcakir, O.; Siemiarczuk, A.; Tutas, M.; Akkaya, E. U. *New J. Chem.* **2010**, *34*, 151–155.
34. Zhang, X.; Xiao, Y.; Qian, X. *Org. Lett.* **2008**, *10*, 29–32.
35. Holten, D.; Bocian, D. F.; Lindsey, J. S. *Acc. Chem. Res.* **2002**, *35*, 57–69.
36. Wagner, R. W.; Lindsey, J. S. *J. Am. Chem. Soc.* **1994**, *116*, 9759–9760.
37. Wagner, R. W.; Lindsey, J. S.; Seth, J.; Palaniappan, V.; Bocian, D. F. *J. Am. Chem. Soc.* **1996**, *118*, 3996–3997.
38. Li, F.; Yang, S. I.; Ciringh, Y.; Seth, J.; Martin Ii, C. H.; Singh, D. L.; Kim, D.; Birge, R. R.; Bocian, D. F.; Holten, D.; Lindsey, J. S. *J. Am. Chem. Soc.* **1998**, *120*, 10001–10017.
39. Ravikanth, M.; Agarwal, N.; Kumaresan, D. *Chem. Lett.* **2000**, 836–837.
40. Kumaresan, D.; Agarwal, N.; Gupta, I.; Ravikanth, M. *Tetrahedron* **2002**, *58*, 5347–5356.
41. Kumaresan, D.; Gupta, I.; Ravikanth, M. *Tetrahedron Lett.* **2001**, *42*, 8547–8550.
42. Lee, C. Y.; Jang, J. K.; Kim, C. H.; Jung, J.; Park, B. K.; Park, J.; Choi, W.; Han, Y. K.; Joo, T.; Park, J. T. *Chem.—Eur. J.* **2010**, *16*, 5586–5599.
43. Ulrich, G.; Ziessel, R. *Tetrahedron Lett.* **2004**, *45*, 1949–1953.
44. Ulrich, G.; Ziessel, R. *J. Org. Chem.* **2004**, *69*, 2070–2083.
45. Ulrich, G.; Ziessel, R. *Synlett* **2004**, 439–444.
46. Goze, C.; Ulrich, G.; Charbonniere, L.; Cesario, M.; Prange, T.; Ziessel, R. *Chem.—Eur. J.* **2003**, *9*, 3748–3755.
47. Galletta, M.; Campagna, S.; Quesada, M.; Ulrich, G.; Ziessel, R. *Chem. Commun.* **2005**, 4222–4224.
48. Galletta, M.; Puntoriero, F.; Campagna, S.; Chiorboli, C.; Quesada, M.; Goeb, S.; Ziessel, R. *J. Phys. Chem. A* **2006**, *110*, 4348–4358.
49. Odobel, F.; Zabri, H. *Inorg. Chem.* **2005**, *44*, 5600–5611.
50. Harriman, A.; Rostron, J. P.; Cesario, M.; Ulrich, G.; Ziessel, R. *J. Phys. Chem. A* **2006**, *110*, 7994–8002.
51. Nastasi, F.; Puntoriero, F.; Campagna, S.; Diring, S.; Ziessel, R. *Phys. Chem. Chem. Phys.* **2008**, *10*, 3982–3986.
52. Nastasi, F.; Puntoriero, F.; Campagna, S.; Olivier, J. H.; Ziessel, R. *Phys. Chem. Chem. Phys.* **2010**, *12*, 7392–7402.
53. Yin, X.; Li, Y.; Li, Y.; Zhu, Y.; Tang, X.; Zheng, H.; Zhu, D. *Tetrahedron* **2009**, *65*, 8373–8377.
54. Rao, M. R.; Kumar, K. V. P.; Ravikanth, M. *J. Organomet. Chem.* **2010**, *695*, 863–869.
55. Wijesinghe, C. A.; El-Khouly, M. E.; Blakemore, J. D.; Zandler, M. E.; Fukuzumi, S.; D'Souza, F. *Chem. Commun.* **2010**, 3301–3303.
56. Benniston, A. C.; Harriman, A.; Whittle, V. L.; Zelzer, M.; Harrington, R. W.; Clegg, W. *Photochem. Photobiol. Sci.* **2010**, *9*, 1009–1017.
57. Sunahara, H.; Urano, Y.; Kojima, H.; Nagano, T. *J. Am. Chem. Soc.* **2007**, *129*, 5597–5604.
58. Wan, C. W.; Burghart, A.; Chen, J.; Bergström, F.; Johansson, L. B. A.; Wolford, M. F.; Kim, T. G.; Topp, M. R.; Hochstrasser, R. M.; Burgess, K. *Chem.—Eur. J.* **2003**, *9*, 4430–4441.
59. Harriman, A.; Izzet, G.; Ziessel, R. *J. Am. Chem. Soc.* **2006**, *128*, 10868–10875.
60. Alamiry, M. A. H.; Harriman, A.; Mallon, L. J.; Ulrich, G.; Ziessel, R. *Eur. J. Org. Chem.* **2008**, 2774–2782.
61. Goeb, S.; Ziessel, R. *Org. Lett.* **2007**, *9*, 737–740.
62. Harriman, A.; Mallon, L.; Ziessel, R. *Chem.—Eur. J.* **2008**, *14*, 11461–11473.
63. Harriman, A.; Mallon, L. J.; Goeb, S.; Ulrich, G.; Ziessel, R. *Chem.—Eur. J.* **2009**, *15*, 4553–4564.
64. Goeb, S.; Ziessel, R. *Tetrahedron Lett.* **2008**, *49*, 2569–2574.
65. Harriman, A.; Mallon, L. J.; Elliot, K. J.; Haefele, A.; Ulrich, G.; Ziessel, R. *J. Am. Chem. Soc.* **2009**, *131*, 13375–13386.
66. Burghart, A.; Thoresen, L. H.; Chen, J.; Burgess, K.; Bergstrom, F.; Johansson, L. B. A. *Chem. Commun.* **2000**, 2203–2204.
67. Bozdemir, O. A.; Cakmak, Y.; Sozmen, F.; Ozdemir, T.; Siemiarczuk, A.; Akkaya, E. U. *Chem.—Eur. J.* **2010**, *16*, 6346–6351.
68. Puntoriero, F.; Nastasi, F.; Campagna, S.; Bura, T.; Ziessel, R. *Chem.—Eur. J.* **2010**, *16*, 8832–8845.
69. Diring, S.; Puntoriero, F.; Nastasi, F.; Campagna, S.; Ziessel, R. *J. Am. Chem. Soc.* **2009**, *131*, 6108–6110.
70. Banuelos, J.; Arbeloa, F. L.; Arbeloa, T.; Salleres, S.; Amat-Guerri, F.; Liras, M.; Arbeloa, I. L. *J. Phys. Chem. A* **2008**, *112*, 10816–10822.
71. Barin, G.; Yilmaz, M. D.; Akkaya, E. U. *Tetrahedron Lett.* **2009**, *50*, 1738–1740.
72. Hagfeldt, A.; Gratzel, M. *Acc. Chem. Res.* **2000**, *33*, 269–277.
73. O'Regan, B.; Gratzel, M. *Nature* **1991**, *353*, 737–740.
74. Erten-Ela, S.; Yilmaz, M. D.; Icli, B.; Dede, Y.; Icli, S.; Akkaya, E. U. *Org. Lett.* **2008**, *10*, 3299–3302.
75. Kolemen, S.; Cakmak, Y.; Erten-Ela, S.; Altay, Y.; Brendel, J.; Thelakkat, M.; Akkaya, E. U. *Org. Lett.* **2010**, *12*, 3812–3815.
76. Kumaresan, D.; Thummel, R. P.; Bura, T.; Ulrich, G.; Ziessel, R. *Chem.—Eur. J.* **2009**, *15*, 6335–6339.
77. Lee, C. Y.; Hupp, J. T. *Langmuir* **2010**, *26*, 3760–3765.
78. Hall, J. D.; McLean, T. M.; Smalley, S. J.; Waterland, M. R.; Telfer, S. G. *Dalton Trans.* **2010**, *39*, 437–445.
79. Peumans, P.; Yakimov, A.; Forrest, S. R. *J. Appl. Phys.* **2003**, *93*, 3693–3723.
80. Walzer, K.; Mannig, B.; Pfeiffer, M.; Leo, K. *Chem. Rev.* **2007**, *107*, 1233–1271.
81. Brabec, C. J.; Sariciftci, N. S.; Hummelen, J. C. *Adv. Funct. Mater.* **2001**, *11*, 15–26.
82. Hummelen, J. C.; Knight, B. W.; Lepeq, F.; Wudl, F.; Yao, J.; Wilkins, C. L. *J. Org. Chem.* **1995**, *60*, 532–538.
83. Li, G.; Shrotriya, V.; Huang, J.; Yao, Y.; Moriarty, T.; Emery, K.; Yang, Y. *Nature Mater.* **2005**, *4*, 864–868.
84. Ma, W.; Yang, C.; Gong, X.; Lee, K.; Heeger, A. J. *Adv. Funct. Mater.* **2005**, *15*, 1617–1622.
85. Reyes-Reyes, M.; Kim, K.; Carroll, D. L. *Appl. Phys. Lett.* **2005**, *87*, 1–3.
86. Bailey, S. T.; Lokey, G. E.; Hanes, M. S.; Shearer, J. D. M.; McLafferty, J. B.; Beaumont, G. T.; Baseler, T. T.; Layhue, J. M.; Broussard, D. R.; Zhang, Y. Z.; Wittmershaus, B. P. *Sol. Energy Mater. Sol. Cells* **2007**, *91*, 67–75.
87. Rousseau, T.; Cravino, A.; Bura, T.; Ulrich, G.; Ziessel, R.; Roncali, J. *Chem. Commun.* **2009**, 1673–1675.
88. Kronenberg, N. M.; Deppisch, M.; Warthner, F.; Lademann, H. W. A.; Deing, K.; Meerholz, K. *Chem. Commun.* **2008**, 6489–6491.
89. Roncali, J.; Leriche, P.; Cravino, A. *Adv. Mater.* **2007**, *19*, 2045–2060.
90. Lloyd, M. T.; Anthony, J. E.; Malliaras, G. G. *Mater. Today* **2007**, *10*, 34–41.
91. Rousseau, T.; Cravino, A.; Bura, T.; Ulrich, G.; Ziessel, R.; Roncali, J. *J. Mater. Chem.* **2009**, *19*, 2298–2300.
92. Rousseau, T.; Cravino, A.; Ripaud, E.; Leriche, P.; Rihn, S.; De Nicola, A.; Ziessel, R.; Roncali, J. *Chem. Commun.* **2010**, 5082–5084.
93. Pavlopoulos, T. G.; Boyer, J. H.; Shah, M.; Thangaraj, K.; Soong, M.-L. *Appl. Opt.* **1990**, *29*, 3885–3886.
94. Shah, M.; Thangaraj, K.; Mou-Ling Soong, M. L.; Wolford, L. T.; Boyer, J. H.; Politzer, I. R.; Pavlopoulos, T. G. *Heteroat. Chem.* **1990**, *1*, 389–399.
95. Drexhage, K. H. Structure and Properties of Laser Dyes In *Topics in Applied Physics*; Schafer, F. P., Ed.; Dye Lasers; Springer: Berlin, 1990; Vol. 1; p 162.
96. Boyer, J. H.; Haag, A. M.; Sathyomoorthi, G.; Soong, M. L.; Thangaraj, K. *Heteroat. Chem.* **1993**, *4*, 39–49.
97. Sathyamoorthi, G.; Boyer, J. H.; Allik, T. H.; Chandra, S. *Heteroat. Chem.* **1994**, *5*, 403–407.
98. Liras, M.; Prieto, J. B.; Pintado-Sierra, M.; Arbeloa, F. L.; Garca-Moreno, I.; Costela, Á; Infantes, L.; Sastre, R.; Amat-Guerri, F. *Org. Lett.* **2007**, *9*, 4183–4186.
99. Ortiz, M. J.; Garcia-Moreno, I.; Agarrabeitia, A. R.; Duran-Sampedro, G.; Costela, A.; Sastre, R.; Lopez Arbeloa, F.; Baouelos Prieto, J.; Lopez Arbeloa, I. *Phys. Chem. Chem. Phys.* **2010**, *12*, 7804–7811.
100. Garcia-Moreno, I.; Zhang, D.; Costela, E.; Martin, V.; Sastre, R.; Xiao, Y. *J. Appl. Phys.* **2010**, *107*.
101. Garcia, O.; Sastre, R.; Del Agua, D.; Costela, A.; Garcia-Moreno, I.; Lopez Arbeloa, F.; Baouelos Prieto, J.; Lopez Arbeloa, I. *J. Phys. Chem. C* **2007**, *111*, 1508–1516.
102. Costela, A.; Garcia-Moreno, I.; Sastre, R.; Lopez Arbeloa, F.; Lopez Arbeloa, T.; Lopez Arbeloa, I. *Appl. Phys. B* **2001**, *73*, 19–24.
103. García, O.; Sastre, R.; Agua, D. d.; Costela, A.; García-Moreno, I.; Roig, A. *Chem. Phys. Lett.* **2006**, *427*, 375–378.
104. Costela, A.; García-Moreno, I.; Gómez, C.; García, O.; Sastre, R. *Chem. Phys. Lett.* **2003**, *369*, 656–661.
105. Canva, M.; Georges, P.; Perelgritz, J.-F.; Brum, A.; Chaput, F.; Boilot, J.-P. *Appl. Opt.* **1995**, *34*, 428–431.
106. Faloss, M.; Canva, M.; Georges, P.; Brun, A.; Chaput, F.; Boilot, J. P. *Appl. Opt.* **1997**, *36*, 6760–6763.
107. Rahn, M. D.; King, T. A.; Gorman, A. A.; Hamblett, I. *Appl. Opt.* **1997**, *36*, 5862–5871.
108. Costela, A.; Garcia-Moreno, I.; Gomez, C.; Garcia, O.; Sastre, R. *J. Appl. Phys.* **2001**, *90*, 3159–3166.
109. Costela, A.; Garcia-Moreno, I.; Pintado-Sierra, M.; Amat-Guerri, F.; Liras, M.; Sastre, R.; Arbeloa, F. L.; Prieto, J. B.; Arbeloa, I. L. *J. Photochem. Photobiol., A* **2008**, *198*, 192–199.
110. Garcia-Moreno, I.; Amat-Guerri, F.; Liras, M.; Costela, A.; Infantes, L.; Sastre, R.; Arbeloa, F. L.; Prieto, J. B.; Arbeloa, A. L. *Adv. Funct. Mater.* **2007**, *17*, 3088–3098.
111. Alvarez, M.; Costela, A.; Garcia-Moreno, I.; Amat-Guerri, F.; Liras, M.; Sastre, R.; Lopez Arbeloa, F.; Baouelos Prieto, J.; Lopez Arbeloa, I. *Photochem. Photobiol. Sci.* **2008**, *7*, 802–813.
112. Garcia-Moreno, I.; Costela, A.; Campo, L.; Sastre, R.; Amat-Guerri, F.; Liras, M.; Lopez Arbeloa, F.; Baouelos Prieto, J.; Lopez Arbeloa, I. *J. Phys. Chem. A* **2004**, *108*, 3315–3323.
113. Costela, A.; Garcia-Moreno, I.; Pintado-Sierra, M.; Amat-Guerri, F.; Sastre, R.; Liras, M.; Lopez Arbeloa, F.; Baouelos Prieto, J.; Lopez Arbeloa, I. *J. Phys. Chem. A* **2009**, *113*, 8118–8124.
114. Lai, R. Y.; Bard, A. J. *J. Phys. Chem. B* **2003**, *107*, 5036–5042.
115. Strangi, G.; Ferjani, S.; Barna, V.; De Luca, A.; Versace, C.; Scaramuzza, N.; Bartolino, R. *Opt. Express* **2006**, *14*, 7737–7744.
116. Veltri, A.; Infusino, M.; Ferjani, S.; Strangi, G. *Mol. Cryst. Liq. Cryst.* **2008**, *488*, 317–326.
117. Ferjani, S.; Barna, V.; De Luca, A.; Versace, C.; Scaramuzza, N.; Bartolino, R.; Strangi, G. *Appl. Phys. Lett.* **2006**, *89*.
118. Ferjani, S.; Barna, V.; De Luca, A.; Versace, C.; Strangi, G. *Opt. Lett.* **2008**, *33*, 557–559.
119. De Luca, A.; Barna, V.; Ferjani, S.; Caputo, R.; Versace, C.; Scaramuzza, N.; Bartolino, R.; Umeton, C.; Strangi, G. *J. Nonlinear Opt. Phys. Mater.* **2009**, *18*, 349–365.
120. Zhu, M.; Jiang, L. I.; Yuan, M.; Liu, X.; Ouyang, C.; Zheng, H.; Yin, X.; Zuo, Z.; Liu, H.; Li, Y. *J. Poly. Sci. A* **2008**, *46*, 7401–7410.
121. Alemdaroglu, F. E.; Alexander, S. C.; Ji, D.; Prusty, D. K.; Borsch, M.; Herrmann, A. *Macromolecules* **2009**, *42*, 6529–6536.
122. Donuru, V. R.; Vegesna, G. K.; Velayudham, S.; Green, S.; Liu, H. *Chem. Mater.* **2009**, *21*, 2130–2138.
123. Donuru, V. R.; Vegesna, G. K.; Velayudham, S.; Meng, G.; Liu, H. *J. Poly. Sci. A* **2009**, *47*, 5354–5366.
124. Kim, B.; Ma, B.; Donuru, V. R.; Liu, H.; Frechet, J. M. J. *Chem. Commun.* **2010**, 4148–4150.

125. Meng, G.; Velayudham, S.; Smith, A.; Luck, R.; Liu, H. *Macromolecules* **2009**, *42*, 1995–2001.
126. Huh, J. O.; Do, Y.; Lee, M. H. *Organometallics* **2008**, *27*, 1022–1025.
127. Nagai, A.; Chujo, Y. *Macromolecules* **2010**, *43*, 193–200.
128. Nagai, A.; Miyake, J.; Kokado, K.; Nagata, Y.; Chujo, Y. *J. Am. Chem. Soc.* **2008**, *130*, 15276–15278.
129. Nagai, A.; Kokado, K.; Miyake, J.; Chujo, Y. *Polym. J.* **2010**, *42*, 37–42.
130. Kajiwara, Y.; Nagai, A.; Chujo, Y. *J. Mater. Chem.* **2010**, *20*, 2985–2992.
131. Nagai, A.; Kokado, K.; Miyake, J.; Cyujo, Y. *J. Poly. Sci. A* **2010**, *48*, 627–634.
132. Nagai, A.; Kokado, K.; Miyake, J.; Chujo, Y. *Macromolecules* **2009**, *42*, 5446–5452.
133. Wang, D.; Miyamoto, R.; Shiraishi, Y.; Hirai, T. *Langmuir* **2009**, *25*, 13176–13182.
134. Bozdemir, O. A.; Bokcakir, O.; Akkaya, E. U. *Chem.—Eur. J.* **2009**, *15*, 3830–3838.
135. Cihaner, A.; Algi, F. *Electrochim. Acta* **2008**, *54*, 786–792.
136. Algi, F.; Cihaner, A. *Org. Electron.* **2009**, *10*, 453–458.
137. Cihaner, A.; Algi, F. *React. Funct. Polym.* **2009**, *69*, 62–67.
138. Camerel, F.; Bonardi, L.; Ulrich, G.; Charbonniare, L.; Donnio, B.; Bourgogne, C.; Guillon, D.; Retailleau, P.; Ziessel, R. *Chem. Mater.* **2006**, *18*, 5009–5021.
139. Camerel, F.; Bonardi, L.; Schmutz, M.; Ziessel, R. *J. Am. Chem. Soc.* **2006**, *128*, 4548–4549.
140. Sartin, M. M.; Camerel, F.; Ziessel, R.; Bard, A. J. *J. Phys. Chem. C* **2008**, *112*, 10833–10841.
141. Ziessel, R.; Bonardi, L.; Retailleau, P.; Camerel, F. *C. R. Chim.* **2008**, *11*, 716–733.
142. Bonardi, L.; Kanaan, H.; Camerel, F.; Jolinat, P.; Retailleau, P.; Ziessel, R. *Adv. Funct. Mater.* **2008**, *18*, 401–413.
143. Wilson, C. J.; James, L.; Mehl, G. H.; Boyle, R. W. *Chem. Commun.* **2008**, 4582–4584.
144. Frein, S.; Camerel, F.; Ziessel, R.; Barbera, J.; Deschenaux, R. *Chem. Mater.* **2009**, *21*, 3950–3959.
145. Camerel, F.; Ulrich, G.; Barbera, J.; Ziessel, R. *Chem.—Eur. J.* **2007**, *13*, 2189–2200.
146. Olivier, J. H.; Camerel, F.; Ulrich, G.; Barbera, J.; Ziessel, R. *Chem.—Eur. J.* **2010**, *16*, 7134–7142.
147. Higgins, D. A.; Liao, X.; Hall, J. E.; Mei, E. *J. Phys. Chem. B* **2001**, *105*, 5874–5882.
148. Bozdemir, O. A.; Guliyev, R.; Buyukcakir, O.; Selcuk, S.; Kolemen, S.; Gulseren, G.; Nalbantoglu, T.; Boyaci, H.; Akkaya, E. U. *J. Am. Chem. Soc.* **2010**, *132*, 8029–8036.
149. Nierth, A.; Kobitski, A. Y.; Ulrich Nienhaus, G.; Jaschke, A. *J. Am. Chem. Soc.* **2010**, *132*, 2646–2654.
150. Qian, X.; Xiao, Y.; Xu, Y.; Guo, X.; Qian, J.; Zhu, W. *Chem. Commun.* **2010**, 6418–6436.
151. Domaille, D. W.; Zeng, L.; Chang, C. J. *J. Am. Chem. Soc.* **2010**, *132*, 1194–1195.
152. Dodani, S. C.; He, Q.; Chang, C. J. *J. Am. Chem. Soc.* **2009**, *131*, 18020–18021.
153. Jiao, L.; Li, J.; Zhang, S.; Wei, C.; Hao, E.; Vicente, M. G. H. *New J. Chem.* **2009**, *33*, 1888–1893.
154. Lee, J. S.; Kang, N. Y.; Yun, K. K.; Samanta, A.; Feng, S.; Hyeong, K. K.; Vendrell, M.; Jung, H. P.; Chang, Y. T. *J. Am. Chem. Soc.* **2009**, *131*, 10077–10082.

Biographical sketch

Ross W. Boyle received his B.Sc. (Hons) in Chemistry and Ph.D. in Organic Chemistry from Paisley College of Technology under the supervision of Professor T.G. Truscott. Following this he spent six years in Canada, first as a postdoctoral research fellow in the MRC Group in Radiation Sciences, University of Sherbrooke with Professor J.E. van Lier, and then at the Department of Chemistry, University of British Columbia, working with Professor D. Dolphin. In 1996 he took up his first academic post as Lecturer in Bioorganic Chemistry at University of Essex and in 2000 he moved to his current post of Reader in Biological Chemistry at Department of Chemistry, University of Hull. Research interests include porphyrin synthetic chemistry, photodynamic therapy, and the application of light active molecules to image and modify biological systems.

Michael Benstead was born in Scarborough, U.K. He received his MChem from the University of Hull in 2007 before carrying out his Ph.D. studies under the supervision of Dr. Ross W. Boyle. His research focussed on the synthesis of BODIPY-based liquid crystals. He completed his Ph.D. in 2010 and is currently working as a postdoctoral researcher at the University of Manchester where his work focuses on poly(aryl ether ketones) (PAEKs).

Georg Mehl obtained his Ph.D. at the University of Freiburg (Germany) in the group of Professor H. Finkelmann. He joined the LC group in Hull as a Post-Doc (with Professor J.W. Goodby), became Lecturer in 1997, DERA Lecturer in 1998 and he is currently a Reader in Supermolecular Chemistry. His research interests are in functional soft self assembling systems, particularly, nano-structured organic–inorganic hybrids, LC nanoparticles, dendrimers and photoactive systems. In the context of LC research he is currently interested in nematic biaxiality.